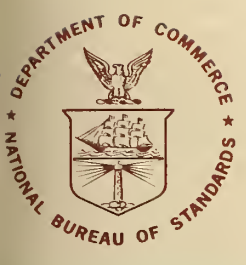

NBS TECHNICAL NOTE 594-11

U.S. DEPARTMENT OF COMMERCE / National Bureau of Standards

Optical Radiation Measurements:

Development of an NBS Reference Spectrophotometer for Diffuse Transmittance and Reflectance

NATIONAL BUREAU OF STANDARDS

The National Bureau of Standards [1] was established by an act of Congress March 3, 1901. The Bureau's overall goal is to strengthen and advance the Nation's science and technology and facilitate their effective application for public benefit. To this end, the Bureau conducts research and provides: (1) a basis for the Nation's physical measurement system, (2) scientific and technological services for industry and government, (3) a technical basis for equity in trade, and (4) technical services to promote public safety. The Bureau consists of the Institute for Basic Standards, the Institute for Materials Research, the Institute for Applied Technology, the Institute for Computer Sciences and Technology, and the Office for Information Programs.

THE INSTITUTE FOR BASIC STANDARDS provides the central basis within the United States of a complete and consistent system of physical measurement; coordinates that system with measurement systems of other nations; and furnishes essential services leading to accurate and uniform physical measurements throughout the Nation's scientific community, industry, and commerce. The Institute consists of the Office of Measurement Services, the Office of Radiation Measurement and the following Center and divisions:

Applied Mathematics — Electricity — Mechanics — Heat — Optical Physics — Center for Radiation Research: Nuclear Sciences; Applied Radiation — Laboratory Astrophysics [2] — Cryogenics [2] — Electromagnetics [2] — Time and Frequency [2].

THE INSTITUTE FOR MATERIALS RESEARCH conducts materials research leading to improved methods of measurement, standards, and data on the properties of well-characterized materials needed by industry, commerce, educational institutions, and Government; provides advisory and research services to other Government agencies; and develops, produces, and distributes standard reference materials. The Institute consists of the Office of Standard Reference Materials, the Office of Air and Water Measurement, and the following divisions:

Analytical Chemistry — Polymers — Metallurgy — Inorganic Materials — Reactor Radiation — Physical Chemistry.

THE INSTITUTE FOR APPLIED TECHNOLOGY provides technical services to promote the use of available technology and to facilitate technological innovation in industry and Government; cooperates with public and private organizations leading to the development of technological standards (including mandatory safety standards), codes and methods of test; and provides technical advice and services to Government agencies upon request. The Institute consists of the following divisions and Centers:

Standards Application and Analysis — Electronic Technology — Center for Consumer Product Technology: Product Systems Analysis; Product Engineering — Center for Building Technology: Structures, Materials, and Life Safety; Building Environment; Technical Evaluation and Application — Center for Fire Research: Fire Science; Fire Safety Engineering.

THE INSTITUTE FOR COMPUTER SCIENCES AND TECHNOLOGY conducts research and provides technical services designed to aid Government agencies in improving cost effectiveness in the conduct of their programs through the selection, acquisition, and effective utilization of automatic data processing equipment; and serves as the principal focus within the executive branch for the development of Federal standards for automatic data processing equipment, techniques, and computer languages. The Institute consists of the following divisions:

Computer Services — Systems and Software — Computer Systems Engineering — Information Technology.

THE OFFICE FOR INFORMATION PROGRAMS promotes optimum dissemination and accessibility of scientific information generated within NBS and other agencies of the Federal Government; promotes the development of the National Standard Reference Data System and a system of information analysis centers dealing with the broader aspects of the National Measurement System; provides appropriate services to ensure that the NBS staff has optimum accessibility to the scientific information of the world. The Office consists of the following organizational units:

Office of Standard Reference Data — Office of Information Activities — Office of Technical Publications — Library — Office of International Relations — Office of International Standards.

---

[1] Headquarters and Laboratories at Gaithersburg, Maryland, unless otherwise noted; mailing address Washington, D.C. 20234.

[2] Located at Boulder, Colorado 80302.

Optical Radiation Measurements:

Development of an NBS Reference Spectrophotometer for Diffuse Transmittance and Reflectance

William H. Venable, Jr., Jack J. Hsia, and
Victor R. Weidner

Optical Physics Division
Institute for Basic Standards
National Bureau of Standards
Washington, D. C. 20234

U.S. DEPARTMENT OF COMMERCE, Elliot L. Richardson, *Secretary*

Edward O. Vetter, *Under Secretary*

Dr. Betsy Ancker-Johnson, *Assistant Secretary for Science and Technology*

NATIONAL BUREAU OF STANDARDS, Ernest Ambler, *Acting Director*

Issued October 1976

National Bureau of Standards Technical Note 594-11

Nat. Bur. Stand. (U.S.), Tech. Note 594-11, 47 pages (Oct. 1976)

CODEN: NBTNAE

U.S. GOVERNMENT PRINTING OFFICE
WASHINGTON: 1976

For sale by the Superintendent of Documents, U.S. Government Printing Office, Washington, D.C. 20402
(Order by SD Catalog No. C13.46:594-11). Stock No. 003-003- **Price $1.15**
(Add 25 percent additional for other than U.S. mailing).

PREFACE

This is the eleventh issue of a series of Technical Notes entitled OPTICAL RADIATION MEASUREMENTS. The series will consist primarily of reports of progress in, or details of, research conducted in radiometry, photometry and spectrophotometry in the Optical Radiation Section and the Radiometric Physics Section of the Optical Physics Division.

The level of presentation in OPTICAL RADIATION MEASUREMENTS will be directed at a general technical audience. The equivalent of an undergraduate degree in engineering or physics, plus familiarity with the basic concepts of radiometry and photometry [e.g., G. Bauer, Measurement of Optical Radiations (Focal Press, London, New York, 1965)], should be sufficient for understanding the vast majority of material in this series. Occasionally a more specialized background will be required. Even in such instances, however, a careful reading of the assumptions, approximations, and final conclusions should permit the non-specialist to understand the gist of the argument if not the details.

At times, certain commercial materials and equipment will be identified in this series in order to adequately specify the experimental procedure. In no case does such identification imply recommendation or endorsement by the National Bureau of Standards, nor does it imply that the material or equipment identified is necessarily the best available for the purpose.

Any suggestions readers may have to improve the utility of this series are welcome.

Henry J. Kostkowski, Chief
Optical Radiation Section
National Bureau of Standards

Jack L. Tech, Chief
Radiometric Physics Section
National Bureau of Standards

TABLE OF CONTENTS

TABLE OF CONTENTS (continued) Page

DEVELOPMENT OF AN NBS REFERENCE SPECTROPHOTOMETER FOR DIFFUSE TRANSMITTANCE AND REFLECTANCE

William H. Venable, Jr., Jack J. Hsia and Victor R. Weidner

A new reference spectrophotometer, designed primarily for the analysis of diffuse transmittance and reflectance, has been developed in the Institute for Basic Standards at NBS. The spectrophotometer consists of a broadband monochromator with optional bandpasses of 2, 5, 10, and 20 nanometers. The exit aperture of the monochromator is provided with special mirror optics to collimate and switch the beam for optional use as a reference or sample beam. These collimated beams are directed into a dark room where a variety of sample mounts, light gathering devices, and detectors can be installed. Measurements for which provisions have been made or are being planned include directional-hemispherical reflectance as a function of angle of incidence, diffuse transmittance, haze, and bidirectional reflectance factor. This Technical Note describes the design of the instrument in detail, and gives the results of the performance tests and detailed error analyses which have been carried out to date.

Key Words: Bidirectional reflectance factor; diffuse reflectance, diffuse transmittance, reflectance; spectrophotometry.

I. INTRODUCTION

Improving the accuracy and usefulness of spectrophotometric measurements made throughout the scientific and industrial community is a fundamental purpose of the spectrophotometry group of the Radiometric Physics Section of NBS. One type of spectrophotometric measurement in which a substantial improvement is needed is that of the interaction of light with turbid media. The principal quantities which are to be measured are directional-hemispherical reflectance and transmittance, bidirectional reflectance factor, and bidirectional transmittance factor. However, in order to measure these accurately, one must determine the effects of a number of related parameters such as translucency and reflections at the sample boundaries.

A reference spectrophotometer for diffuse reflectance and transmittance measurements has been constructed at NBS utilizing a modular design and state of the art components. This design allows flexibility in investigating the many aspects of the measurements and it can be adapted to additional types of measurements in the future. The instrument consists of a monochromatic source radiator which projects the radiation into an adjoining darkroom. This radiation source is described in part II of this Technical Note. A number of specialized sample mounts, light gathering devices, and detection systems can be installed in the darkroom for performing specific measurements. For brevity, these will be called the "accessories". Several of them are described in part III. The experiments are controlled and the data is gathered and analyzed by a mini-computer which is interfaced with the instrument using a modular interactive data acquisition system (MIDAS)[1][1] developed in part at NBS [2]. A block diagram showing the general arrangement of the experiment control and data gathering system is shown in figure 1.

---

[1]Figures in brackets indicate the literature references at the end of this paper.

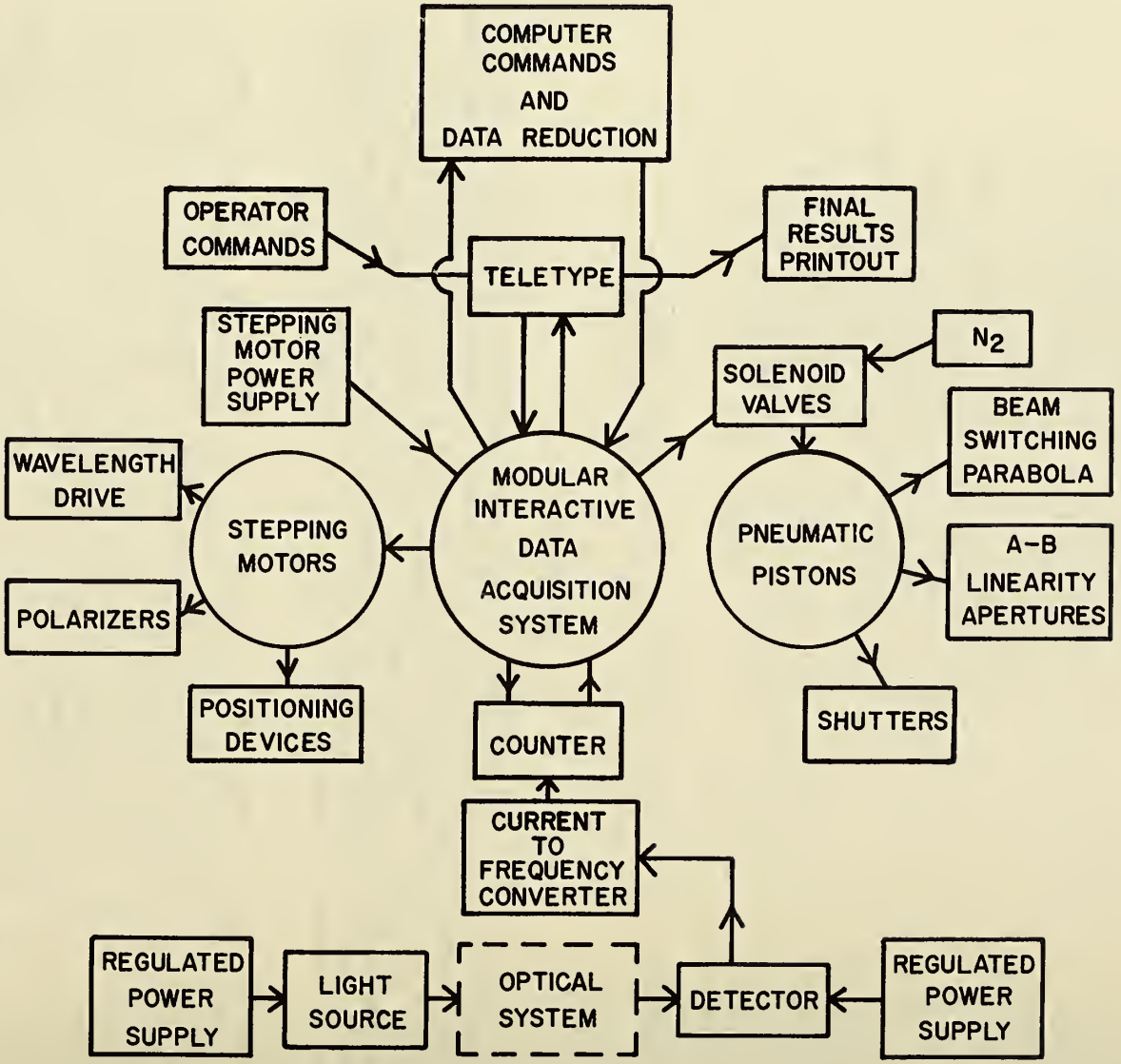

Figure 1. Block diagram for the spectrophotometer and its control system.

II. SPECTROPHOTOMETER DESIGN

The general layout of the optical system of the spectrophotometer is shown in figure 2. The source, alignment laser, and monochromator are mounted on a surface plate with their optic axes horizontal and parallel to the surface of the plate. The exit aperture of the monochromator is attached to a light tight diaphram in a partition that separates the room containing the monochromator and source optics from the dark chamber in which are located the exit aperture optics and the accessories. The accessory pictured in figure 2 is an integrating sphere for directional-hemispherical reflectance measurements. The electronics and control systems are located in the same room as the monochromator, leaving the dark chamber free of all sources of light except the beam from the monochromator. The dark chamber is lined with black felt to absorb stray radiation.

A. Light Sources

The light source ordinarily used with the instrument for the spectral range 400 to 800 nanometers is a tungsten lamp with a 14 mm long by 2 mm wide ribbon filament (GE Microscope Illuminator, T10 bulb, SR-8 filament, 6V, 18A [1]). The tungsten lamp is powered by a regulated supply operated in the constant voltage control mode. This lamp operates in the temperature range of 2100 K to 2900 K. Other sources such as deuterium lamps or xenon arcs can be substituted for operation in the ultraviolet and visible spectral ranges. A helium-neon laser is used to align the optical components in the system. The source and the optical system used to direct the radiation into the monochromator are enclosed in a cover to reduce air currents which can affect the stability of the source.

B. Source Optics

Associated with the light source is an optical bench on which are located mirrors for introducing the radiation into the predisperser and monochromator. The light from the tungsten source is collected and collimated by a 52 mm diameter, 15° off-axis parabolic mirror, having a focal length of 178 mm. The collimated beam of radiation is directed to a flat mirror near the end of the optical bench. The beam is directed by the flat mirror to a second 15° off-axis parabolic mirror which in turn focuses an image of the source on the entrance aperture of the predisperser. The use of mirrors rather than lenses in the system reduces interreflections, improves throughput of radiation in the UV and IR spectral ranges, and eliminates wavelength dependent focusing. The mirrors have been coated with MgF_2 in order to maintain their reflectance to greater than 80% down to 180 nm wavelength. The off-axis parabolic mirrors are mounted in micrometer controlled angular orientation devices which are in turn mounted on micrometer cross fed slides for ease of alignment. Polarizers can be inserted into the collimated beam for controlling the intensity of the light or its plane of polarization. The polarizers are mounted in stepping motor driven rotators for independent programmable rotation of each polarizer in the beam.

The two off-axis parabolic mirrors used in the source optics along with a third off-axis parabolic mirror located at the exit slit of the monochromator were specially made for this instrument. They were tested [3] at 15° off-axis with a shearing interferometer at wavelength 577 nm. Collimated light with wavefront deviations no greater than 1/20 wavelength from a plane wave was incident on the parabolic mirror at an angle of 15° ± 0.25° with respect to the test system optical axis. This arrangement simulated the application for the mirror in which a light source at the mirror focus will produce a nearly collimated light. These mirrors were found to be within the diffraction limited performance desired. (In the strictest sense, off-axis parabolic mirrors cannot be diffraction limited because of their inherent astigmatism and coma.) The mirror focal lengths fell within the ±2 mm tolerances placed on them. The fringe pattern for these three mirrors and two additional mirrors that were prepared from the same parabolic mirror are the same to within 1/10 of a fringe when comparing the superpositioned interferogram negatives.

C. Predisperser

The predisperser is an Ebert prism instrument with a 2 mm entrance slit (McPherson 608M1 [1]). The purpose of the predisperser is to eliminate higher order wavelengths and reduce stray light in the monochromator. It has a range of 180 nm to 2600 nm. The focal length of the collimating and focusing mirrors is 15.2 cm with a horizontal aperture ratio

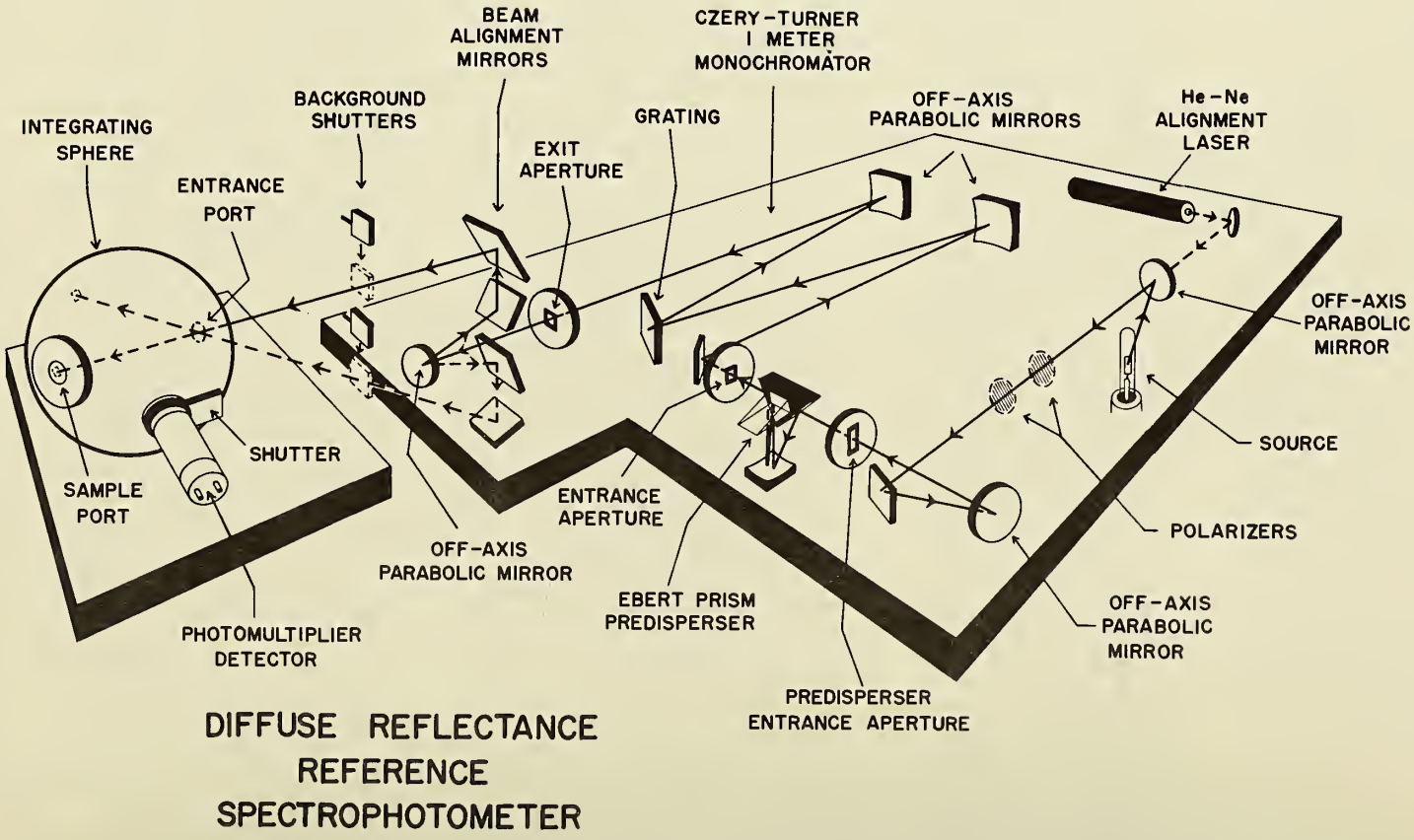

Figure 2. Pictorial diagram of spectrophotometer optical system.

of f/6. The predisperser wavelength drive is synchronized with the wavelength drive of the monochromator.

D. Monochromator

1. Description

The monochromator is a 1-meter Czerny-Turner system with an effective aperture of f/8.7 (McPherson 2051 [1]). Its useful wavelength range is from 200 nm to more than 30 μm with appropriate selection of gratings. The grating presently in use is a plane grating 102 mm by 102 mm having 150 grooves per mm and is blazed at 500 nm. With this grating, the monochromator has a linear dispersion of 6.66 nm/mm.

The monochromator utilizes off-axis parabolic mirrors to collimate the beam on the grating and to focus the dispersed beam on the exit aperture. The entrance and exit apertures of the monochromator are located on rotational devices with four stop positions to allow selection of apertures of 0.300 mm, 0.750 mm, 1.500 mm, and 3.000 mm straight slits corresponding to bandpasses of 2 nm, 5 nm, 10 nm, and 20 nm respectively. The height of the slit can be adjusted from zero to 10 mm. (A larger lamp filament or different source optics would be required for 20 nm band operation.)

The wavelength setting of the monochromator is precise to 0.01 nm. The initial setting of the wavelength scale in an experiment is accomplished by turning the wavelength drive by hand and observing a vernier dial. A stepping motor is used to change the wavelength settings during the experiment. The computer control program is designed to avoid errors due to backlash in the wavelength drive gear train, and at the end of each experiment the wavelength scale is returned to the initial position to allow a check for mechanical slippage.

2. Calibrations and Tests

a. Wavelength calibration -- For measurements in which wavelength is critical, such as the measurement of highly chromatic color samples, the wavelength calibration will be done using stable line emission sources. The general procedure, which has been employed in broadband measurements made with the IBS reference spectrophotometer for transmittance [4], is to scan the monochromator past a source line wavelength and, at regular wavelength intervals, to take readings proportional to the flux transmitted by the monochromator. From these readings, the centroid wavelength scale setting corresponding to the line wavelength can be determined. Since no wavelength-critical measurements have been performed to date with the instrument being described in this Technical Note, it has not been calibrated with line sources.

With the monochromator set at 10 nm bandpass, an NBS Standard didymium glass, calibrated with 10 nm spectral width [5], was employed to check the wavelength scale. The didymium glass was placed in a pneumatically driven slider which was mounted on the optical bench before the predisperser. The slider accommodates one didymium glass plus a clear space, so that the spectral transmittance of the didymium glass can be measured. The measured wavelength of minimum transmittance are listed below with the assigned wavelengths of minimum transmittance for the NBS Standard didymium glass.

Assigned Wavelength (nm)	Overall Uncertainty in Assigned Wavelength (nm)	Measured Wavelength (nm)
441.0	±1.0	440.6
475.5	±1.0	475.8
528.7	±1.0	529.1
585.0	±1.0	585.2
684.8	±1.0	685.0
743.5	±1.0	744.0

The differences between the measured and the assigned wavelengths of minimum transmittance are all within the uncertainty in the assigned values. Therefore it can be assumed from this test that the wavelength scale is accurate at least to within ±1.0 nm.

b. Stray radiant energy -- Stray radiant energy was checked by means of two test methods. The same apertures (1.5 × 1.5 mm) were used for these tests as are used for reflectance measurements with 10 nm bandpass.

The first method is to measure the transmittance of glass filters at the wavelengths for which their transmittance is low. When the value of transmittance does not change when an additional thickness of glass filter is palced in the light beam, then this apparent transmittance is due to the stray radiant energy passed by the filters at other wavelengths where their transmittance is high. The first filter check was made with two selenium orange glasses [6] measured at 400 and 500 nm. The results are as follows:

Wavelength (nm)	Transmittance of One Glass	Transmittance of Two Glasses
400	6.1×10^{-6}	4.1×10^{-6}
500	2.9×10^{-4}	2.4×10^{-4}

Since the transmittance of one filter is approximately 0.9 at wavelengths above 600 nm and nearly zero below 550 nm it follows that with the monochromator set at 400 nm the total stray radiant energy at wavelengths above 600 nm contributes 5×10^{-6} of the detector output due to the total incident radiation. With the wavelength set at 500 nm, the contribution to the detector output by radiation at wavelengths above 600 nm is 3×10^{-4}.

The second filter check was made with four cobalt blue filters [6]. The transmittance measured for three and four filters was found to be:

Wavelength (nm)	Transmittance of Three Glasses	Transmittance of Four Glasses
600	4.6×10^{-5}	4.6×10^{-5}

Each of these filters transmits approximately 0.8 in the wavelength region from 350 nm to 450 nm and approximately 0.9 above 700 nm. The total stray radiant energy in those wavelength ranges contributes approximately 1×10^{-4} of the detector output due to the total incident radiation.

The second type of stray radiation test made use of a helium-neon laser (632.8 nm) as the source of input radiation. Readings of the detector output were made at various wavelength settings of the monochromator. The normalized detector outputs were as follows:

Wavelength Setting (nm)	Normalized Detector Output
400	0.5×10^{-6}
500	3.0×10^{-6}
600	84.0×10^{-6}
632.8	1 (peak)
650	84.0×10^{-6}
700	16.0×10^{-6}
750	1.0×10^{-6}

If it is assumed that a similar performance would occur for incident monochromatic radiation at all other wavelengths, one can calculate that roughly 4×10^{-5} of the radiation passed by the monochromator will be at wavelengths outside the nominal passband. This is in order of magnitude agreement with the values observed with filter glasses.

E. Exit Slit Optics

The exit slit of the monochromator is attached to a light tight diaphragm in a wall so that the emerging radiation enters a 3 by 3 meter dark chamber. A unique feature of the instrument is an optical system located at the exit aperture of the monochromator which is designed to collimate the beam, switch the beam from one of two paths to the other, and provide for directing the beams to the positions required for the various experimental apparatus in the dark chamber. This system is located in the dark chamber, but is supported by a rigid extension of the frame supporting the monochromator surface plate so that its optical alignment remains stable with respect to the monochromator. It is illustrated in figures 2 and 3. (See also appendix G.)

The entire system can be positioned vertically and horizontally by three precision screw driven slides to facilitate its alignment with respect to the monochromator exit slit. The key optical component in this system is a 15° off-axis parabolic mirror 52 mm in diameter. The exit aperture of the monochromator is located near the focal point of the parabola. The parabolis mirror is mounted on a pneumatic device which can rotate the mirror 180° clockwise or counterclockwise in approximately 1/4 second. This enables the collimated beam to be switched from one path to the other. This rotation assembly is mounted on a precision slide for independent vertical alignment. Located just above and below the exit aperture are sets of two flat mirrors that intercept the collimated beam from the parabolic mirror. Each flat mirror closest to the parabolic mirror is adjusted to direct the beam to a second flat mirror. located directly above it. The second flat mirror is mounted on precision slides which provide for up and down displacement of the beams. A rotation adjustment about a horizontal axis on each of these mirrors allows for setting the up and down angular direction of each beam. In addition, three spring washer loaded screws are provided for horizontal alignment of the beam. The emerging beam is approximately 10 mm wide for a 10-nm bandpass and the height is adjustable at the monochromator exit slit.

The accurate 180° rotation of the parabolic mirror is assured by means of a gravity dependent system in which a steel ball on the end of an arm attached to the mirror mounting disk is caused to fall against a stop when the pneumatic piston is triggered to rotate the mirror. When the steel ball is at rest on one stop the beam is directed to the upper mirror; when it is at rest on the second stop, the beam is directed to the lower mirrors. The piston intercepts an arm attached to the axis on which the mirror rotates and lifts the steel ball, flipping the ball over the center of gravity, at which point, gravity causes it to come to rest on the stop. The action of the piston is reversible and it is operated by the experiment control system.

All the mirrors in the exit aperture optics, including the off-axis parabolic mirror are made of Cer-Vit [1] glass having negligible thermal expansion. These mirrors are mounted on invar steel to further reduce mirror distortion due to variation in thermal expansion between the mirror and its mounting.

Also incorporated in the exit aperture system is a shutter consisting of two light traps, attached to the shaft of a pneumatic piston, which can be adjusted to intercept the beam as it leaves the exit aperture mirror system by either path. This shutter, which is used to trap the beam when making background signal measurements, can be moved in and out of the beam by actuating the piston through the experiment control system.

III. MEASUREMENT ACCESSORY SYSTEMS

Because of the modular design of the instrument, the optical system as it exists beyond the exit aperture optics depends upon the measurement being made. For each type of measurement, there is a measurement accessory system which may incorporate sample mounts, radiation gathering devices, and detectors. These are mounted on a platform which can be positioned

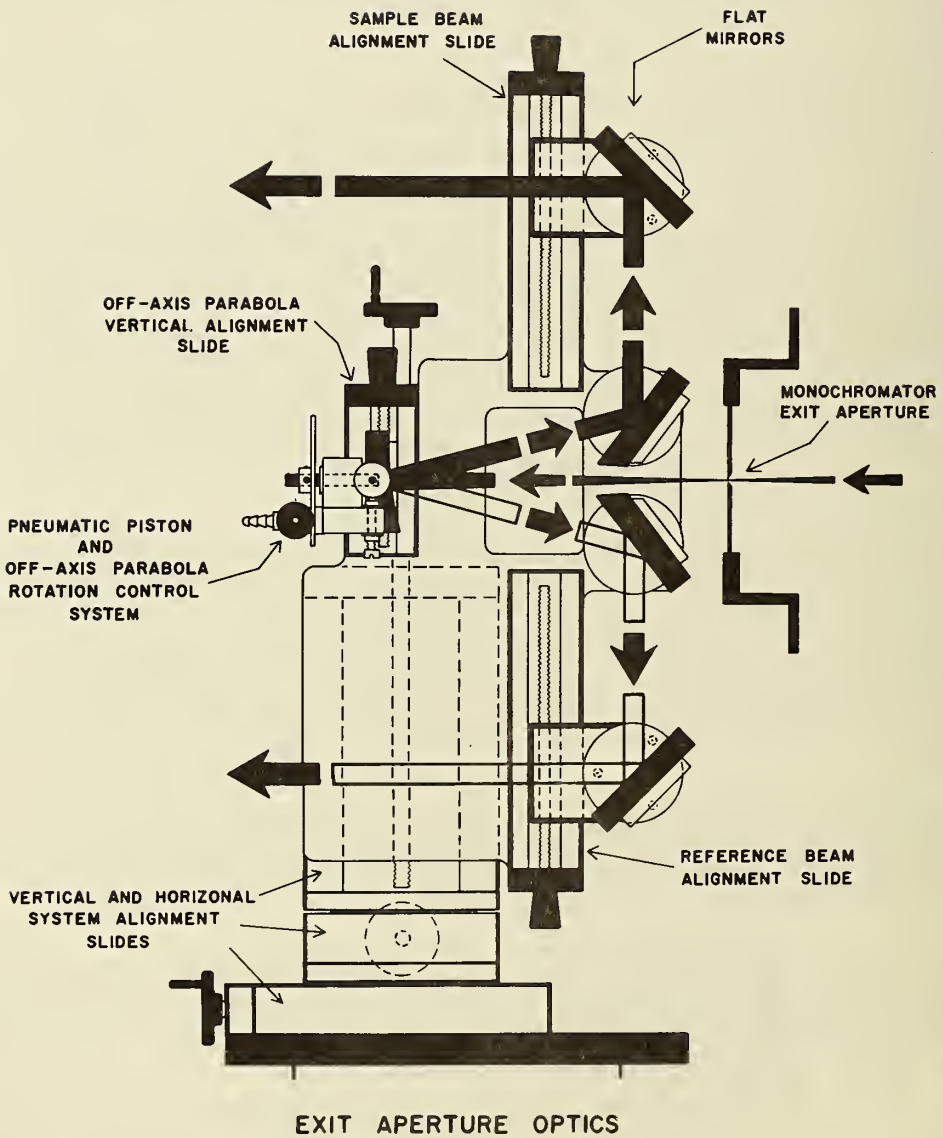

Figure 3. Exit aperture optics and beam switch.

vertically with a lift table and horizontally in both directions by means of ball bushing slides. Stepping motors can be attached to provide automated horizontal positioning as required. In the following sections, several of the measurement accessory systems are described as they now exist or as they are proposed.

A. General Purpose Integrating Spheres

1. Description

Two integrating spheres which are used for measuring directional-hemispherical reflectance are shown in figures 4 and 5. The two spheres are the same except for a variation in the angle at which the beam is incident upon the sample. In one sphere the beam is incident on the sample normal to its surface so that the surface reflection from a high gloss sample returns along the same path in which it entered the sphere and is excluded from the measurement. The other sphere includes most of the surface reflection because the beam is incident on the sample at 6° from normal.

The spheres are approximately 30 cm in diameter. The sample and reference beams enter through the same port, thus reducing the number of openings in the sphere to three: the entrance port, which is 38 mm in diameter; the sample port, which is 50.8 mm; and the detector port, which is approximately 48 mm. The spheres are constructed of two aluminum hemispheres with a white coating of a tetrafluroethylene powder [7,8] called Halon [1]. This coating is applied so as to completely eliminate the seam between the hemispheres, when they are assembled.

The two spheres are mounted together on a pier designed to allow measurements to be made with the specular component included or excluded by rotating either sphere into the position where the sample and reference beams are directed to enter the sphere. The support pier is designed with interchangeable sphere yokes that allow the system to measure samples by mounting them on the sample port in the vertical or horizontal plane. The provision for horizontal mounting of the specimen is to allow for measuring loose powders and liquids. An additional mirror is required to direct the sample and reference beams to the horizontally mounted samples.

The sample port is designed so that the sample surface to be measured is slightly inside the tangent to the curvature of the internal surface of the sphere. The edge of the sample port is only approximately 0.6 mm thick where the inside curvature of the sphere meets the plane of the sample to allow as much of the diffusely reflected radiation as possible to be included in the measurement. The sample beam illuminates an area of the sample approximately 10 mm by 18 mm in the center of the 50.8 mm diameter port. This allows for the complete return of the reflected signal from within most nearly opaque samples without losses caused by the port edge being too close to the area of illumination.

The relationship of the detector port to the entrance and sample ports is shown in figure 6. The detector port is located 90° from the other ports. Direct reflections from the sample port to the detector are prevented by a collar at the detector port. This collar is coated inside and out with the same white material as the sphere wall. A pneumatically operated shutter is located between the white lined collar and the photocathode surface to protect the detector when the room lights are turned on.

The reference beam strikes an area of the sphere near the sample port. The coating on this area is slightly built up so that direct reflection of radiation from this spot to the sample port is prevented. This is required to reduce a slight non-linearity as described in Appendix A.

2. Definition of the Measurement

These accessory spheres are used to determine the ratio of the spectral directional-hemispherical reflectances ρ_x and ρ_y of two flat diffusely reflecting samples x and y. The spectral directional-hemispherical reflectance can be defined generally as

$$\rho_x(\lambda) = \iint S_x(\vec{P},\vec{U};\vec{p},\vec{u},\lambda)\vec{u}\cdot d\vec{a}d\omega \qquad (1)$$

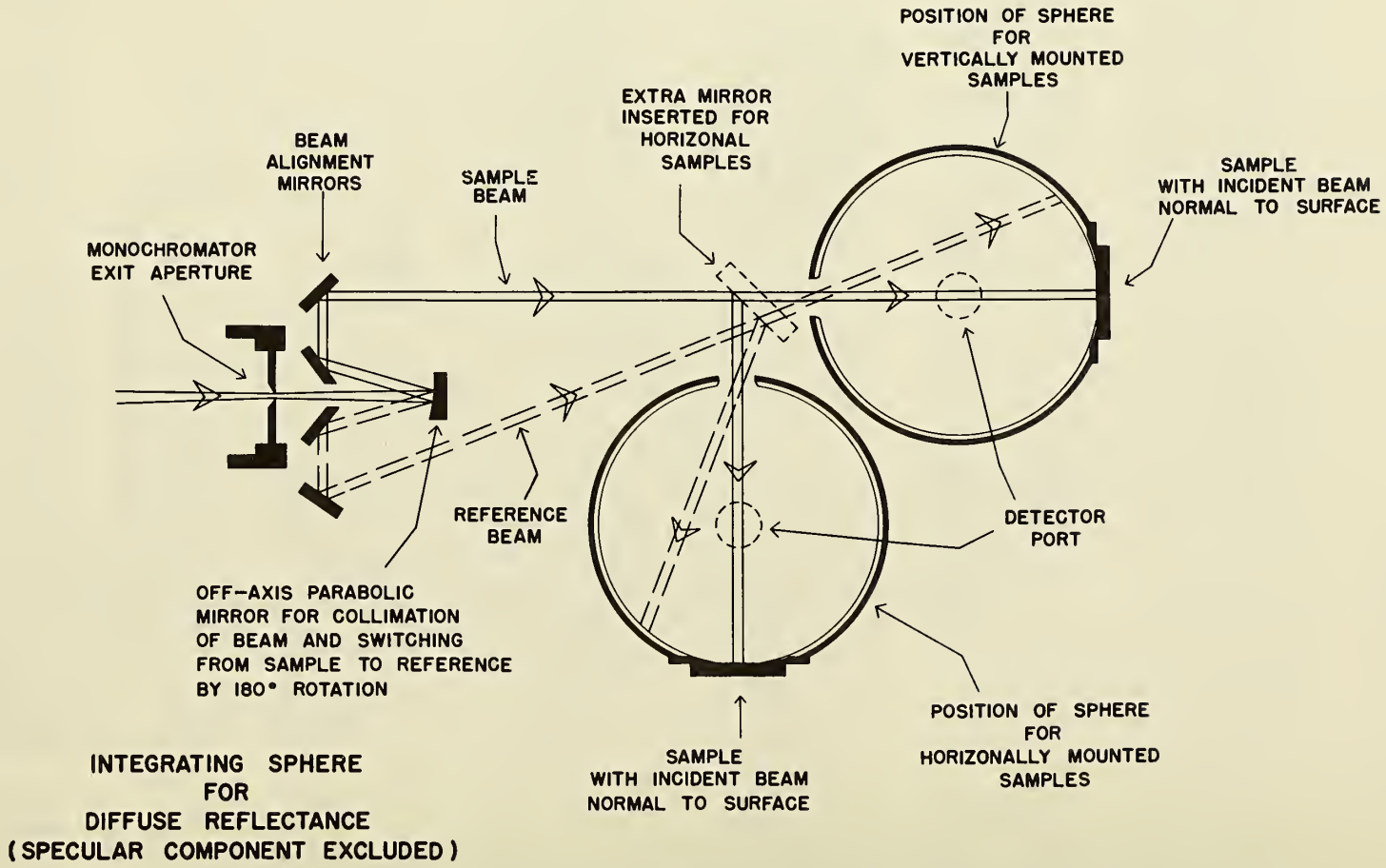

Figure 4. Integrating sphere for directional-hemispherical reflectance with specular component excluded.

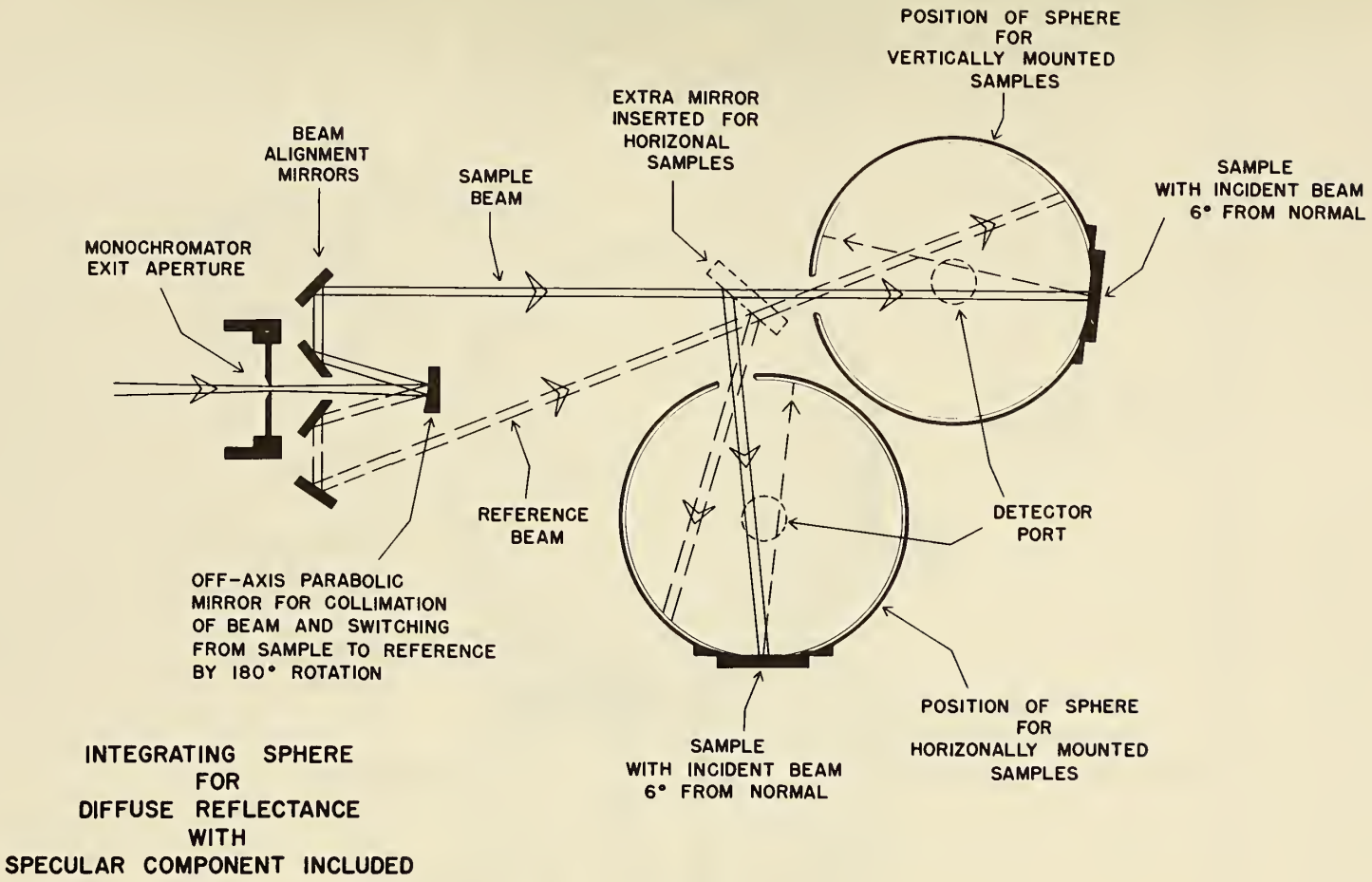

Figure 5. Integrating sphere for directional-hemispherical reflectance with specular component included.

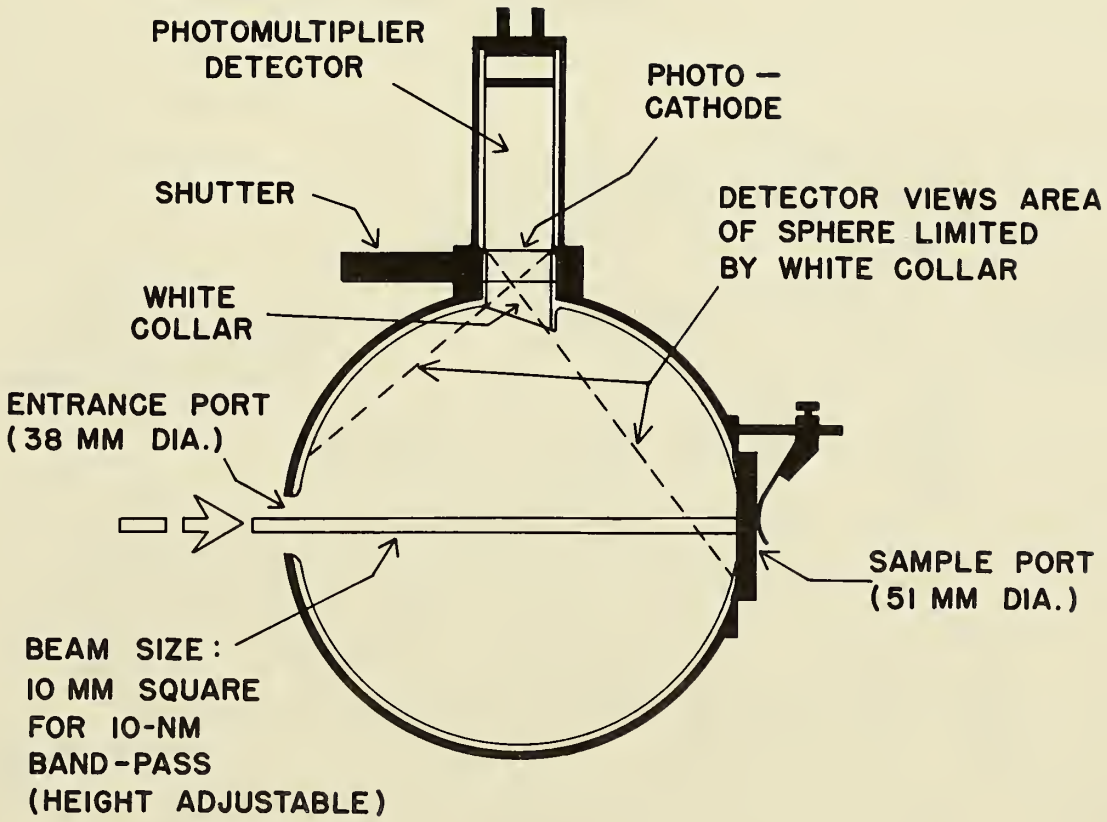

Figure 6. Diffuse reflectance integrating sphere showing detector position.

where $S_x(\vec{P},\vec{U};\vec{p},\vec{u},\lambda)$, the generalized scattering function for sample x, is the radiance emerging in a direction $\vec{u}$ from point $\vec{p}$ on the sample surface resulting from a unit flux incident in direction $\vec{U}$ at point $\vec{P}$ on the sample. These spheres are to be used only for non-fluorescing samples for which S_x is a function only of one wavelength λ. The integral of the reflected radiance is taken with respect to area a over the entire sample surface and with respect to solid angle ω over the entire hemisphere of directions of emergence. (A complete discussion of this approach to defining measurements appears in an earlier Technical Note.[9])

The measurement which is actually made involves the ratio Q_x of two signals, N_x which is obtained from the detector when the incident radiation falls on sample x, and N_w which is obtained when the incident radiation falls on the sphere wall.

$$Q_x = N_x/N_w \tag{2}$$

In terms of the defining notation of reference [9],

$$Q_x = \frac{\iiiiint L_s S_x R_{sx} \vec{U}\cdot d\vec{A} d\Omega \vec{u}\cdot d\vec{a} d\omega d\lambda}{\iiiiint L_w S_w R_{wx} \vec{U}\cdot d\vec{A} d\Omega \vec{u}\cdot d\vec{a} d\omega d\lambda} \tag{3}$$

where $L_s = L_s(U,\underset{\sim}{P},\lambda)$ is the radiance in the sample beam at wavelength λ which strikes the sample at point $\vec{P}$ in direction $\vec{U}$, L_w is a similar expression for the radiance in the reference beam striking the sphere wall, $R_{sx}(\vec{p},\vec{u},\lambda)$ is a function describing the instrument's response to the radiation reflected from the sample, and R_{wx} is a similar expression for the instrument's response to reference beam radiation reflected from the sphere wall. Note that since the sample x is part of the sphere wall, both R_{sx} and R_{wx} depend upon the reflectance of the sample. The measurement assumption is that

$$\frac{\rho_y}{\rho_x} \underset{\sim}{=} \frac{Q_y}{Q_x} . \tag{4}$$

The extent to which the approximation in eq. (4) approaches true equality depends upon a number of factors, some of which will be discussed later in part III.A.4. In some cases, corrections for Q_y/Q_x can be determined which will cause the approximation in eq. (4) to be more reliably near equality. These corrected expressions are given in eqs. (8) and (9).

3. Reflectance Measurement Procedure

Measurements of spectral reflectance are made with these spheres by comparing first, the reflected signal from the sample to the reference beam signal, and then making the same comparison with a reflectance standard in place of the sample.

With the measuring sphere in position and sample x in the sample port, the relative directional-hemispherical reflectance of sample x to the sphere wall is ordinarily determined by the following procedure. The data are recorded for Z, N'_x, N'_w, N'_x, Z and corresponding time t_1, t_2, t_3, t_4, t_5 where N'_x is the detector output signal when the sample beam strikes x; N'_w is the signal when the reference beam strikes the sphere wall; and Z is the dark current reading taken with the background shutters blocking both beams. The measurement sequence above is repeated two more times. Since the parabolic mirror and the shutter in the exit slit optical system are controlled remotely, this sequence of measurements is achieved easily. For each signal, the count from the current-to-frequency converter is integrated over a ten second interval. A waiting period of 10 seconds is allowed after changing the light level before the count is measured in order to allow any effects of electrical transients to subside. A computer program was written to reduce the data in the following manner. If the detection system is found to be non-linear as described in part III.A.4.a, the values of N'_x and N'_w are corrected accordingly. The signals of Z and N'_x are then linearly interpolated with respect to time to obtain a value for each at time t_3. The

relative reflectance Q_x of the sample x is then computed

$$Q_x = \frac{N'_x(t_3) - Z(t_3)}{N'_w(t_3) - Z(t_3)} \tag{5}$$

The same computing procedure is repeated for the other two measurements. The average of the three relative reflectance $\overline{Q}_x$, is computed and the standard error is determined.

$$\overline{Q}_x = (1/3)\ \Sigma Q_x \tag{6}$$

$$\sigma = [\frac{1}{(3)(2)}\ \Sigma(Q_x - \overline{Q}_x)]^{\frac{1}{2}} \tag{7}$$

For highly reflecting sample, a typical value for σ is found to be 2×10^{-4} and is less for a sample with low reflectance. This has been verified by repeated measurements. The values for $\overline{Q}_x$ are used in eq. (4) to calculate the measured ratio of reflectances ρ_y/ρ_x.

4. Evaluation

a. Detector linearity

The linearity of the detector and electronic system was determined by using the light-addition method with a double-aperture apparatus [4,10], that is, the output of the detector system when irradiated by two light beams simultaneously is compared to the sum of the outputs obtained when the detector is irradiated by each light beam separately. Measurements were also made of the signal as a function of time. Two typical cases are shown in figure 7. In both cases, the drift was approximately linear in time over a 30 minute time interval which is sufficient for the requirements of the linearity test. (The slope of the drift-in-time curve was not always negative.)

The non-linearity is less than 0.01 percent of the full-scale reading. The results are presented below together with the standard deviation of the non-linearity determination.

N_m	ΔN	$SD(\Delta N)$
0.1	6.5×10^{-5}	1.2×10^{-5}
0.2	9.3×10^{-5}	2.1×10^{-5}
0.3	9.4×10^{-5}	2.9×10^{-5}
0.4	7.5×10^{-5}	3.7×10^{-5}
0.5	4.5×10^{-5}	4.5×10^{-5}
0.6	1.1×10^{-5}	5.0×10^{-5}
0.7	1.9×10^{-5}	5.0×10^{-5}
0.8	3.6×10^{-5}	4.3×10^{-5}
0.9	3.2×10^{-5}	2.7×10^{-5}
1	0	0

N_m = the measured signal normalized to 1 at a photomultiplier current of 3×10^{-7} A. ΔN = the amount of the linearity correction on the same scale required to make N proportional to the flux striking the detector. $N = N_m + \Delta N$. $SD(\Delta N)$ = the standard deviation of ΔN.

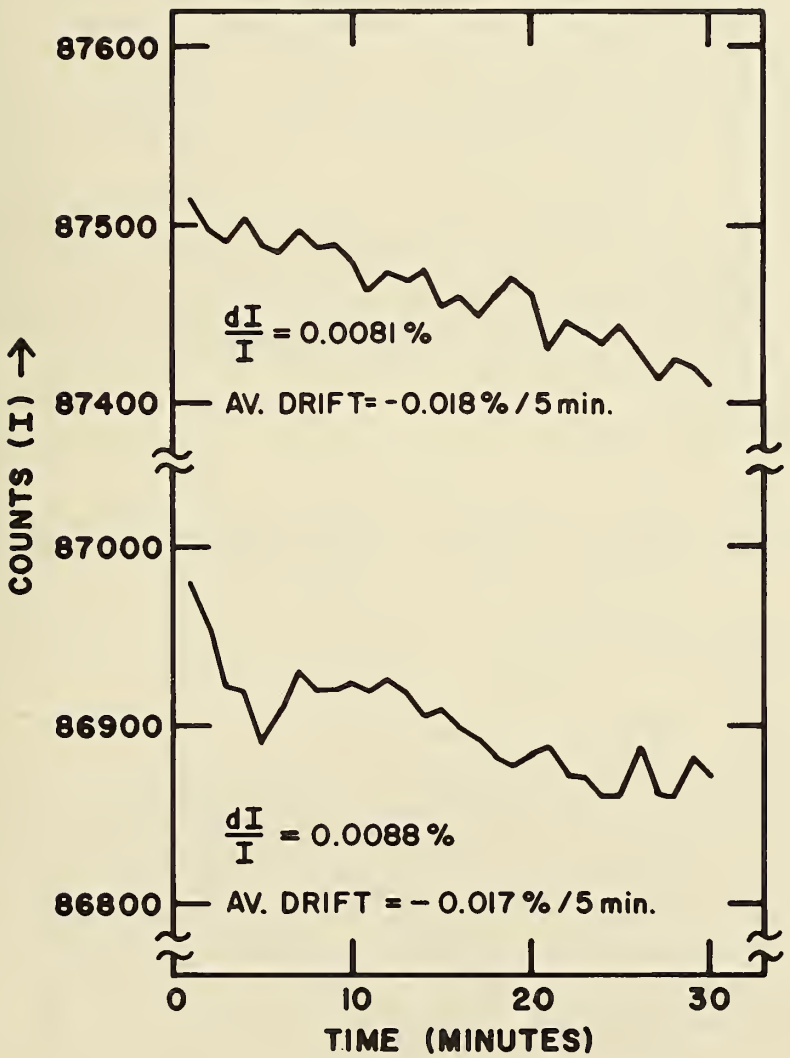

Figure 7. System drift as a function of time.

b. Sample-induced nonlinearity

The magnitude of the responses R_{sx} and R_{wx} in eq. (3) must have the same dependence on S_x if eq. (4) is to approach equality. The departure from this ideal condition will be called sample-induced nonlinearity, and some of its causes are discussed in appendix A. The general purpose measuring sphere with 6° incident angle (specular component included) was tested for sample-induced nonlinearity as described in appendix B. In this appendix, eq. (4) as modified to take sample-induced nonlinearity into account takes on the form:

$$\frac{\rho_y}{\rho_x} \simeq \frac{Q'_y}{Q'_x}\,(1 + \alpha(Q'_x - Q'_y)) \qquad (8)$$

where Q'_x is the relative reflectance of the sample x as measured and α is a correction coefficient. (See final paragraph of appendix B.)

The initial measurements were made with no baffle between the sample port and the point at which the reference beam strikes the wall. In this case, the experimentally determined value of α was found to be -0.0076. In appendix E, it is shown that the value of the contribution to α caused by the sample's being flat is -0.0077. This suggests that the contribution to α due to other causes such as retroreflectance of the sphere wall was either negligible or not detected by the test. When a baffle was introduced between the sample and the incident point for the reference beam, the experimentally determined value of α was found to be 0.002. In this case, the nonlinearity caused by the sample's being flat should have been eliminated, but reflections from the baffle are estimated to contribute .001 to α. The difference between the estimated and measured values of α may be due to the approximate nature of the theory involved in estimating the nonlinearity caused by the baffle reflection or there may be another contributing factor to sample-induced nonlinearity which has not been taken into account. Since there is no reason at present to doubt the results of the nonlinearity test, and since independent tests of the wall retroreflectance have indicated that its contribution to α is an order of magnitude smaller than that of reflections from the baffle, the results of the test will be assumed correct and ratios of reflectance values will be determined using 0.002 for α in eq. (8).

c. Polarization effects

The detection system was tested for sensitivity to polarization of the reflected radiation and was found to be independent of polarization to within the measurement uncertainty of 0.05%. These tests are described in appendix D. The ratio of the signal for source radiation polarized with the electric vector parallel to the monochromator plane to the signal for the same amount of source radiation polarized perpendicular to the monochromator plane was 1.4 at 450 nm and 1.6 at 700 nm. This indicates that the monochromator partially polarizes the radiation it transmits, as would be expected in a grating instrument.

d. Angular dependence of response

The response R_{sx} depends upon the direction of emergence $\vec{u}$ of radiation reflected from the sample. The closer R_{sx} is to being constant, the more eq. (4) can be relied upon to approach equality. In the general purpose measuring spheres, there are two main departures from constant R_{sx}. The first of these is that R_{sx} is zero within the solid angle subtended at the sample by the entrance port. The second results from the structure of the sample port. In order to taper the sphere wall to the sample port, the portion of the sphere wall bounding the sample port is made of aluminum painted white, rather than being Halon.[1] Therefore, the response in the solid angle subtended by this ring is lower than the response of other directions by the ratio of the reflectance ρ_p of the paint to the reflectance ρ_H of the Halon, both reflectances being for grazing incidence.

If both S_x and S_y depend upon $\vec{u}$ in the same way, no error will be introduced by the nonuniformity of R_{sx}. However, if this is not the case, the detailed dependence of both S_x and S_y upon $\vec{u}$ must be used to calculate the error for a given pair of samples. In such a case, a more reliable approximation than eq. (4) to the reflectance ratio could be written as

$$\frac{\rho_y}{\rho_x} \simeq \frac{Q_y}{Q_x}(1 + \varepsilon_p + \varepsilon_r) \tag{9}$$

where

$$\varepsilon_p = \iint \left(\frac{S_y}{\rho_y} - \frac{S_x}{\rho_x}\right) \vec{u}\cdot d\vec{a}\, d\omega \tag{10}$$

where the integral with respect to solid angle ω is taken only over the solid angle subtended at the sample by the entrance port, and

$$\varepsilon_r = \left(1 - \frac{\rho_p}{\rho_H}\right) \iint \left(\frac{S_y}{\rho_y} - \frac{S_x}{\rho_x}\right) \vec{u}\cdot d\vec{a}\, d\omega \tag{11}$$

where the integral with respect to solid angle ω is taken over the solid angle subtended at the sample by the painted ring surrounding the sample port. The projected solid angle subtended at the sample by the entrance port is .013 sr, the projected solid angle subtended by the painted ring is .055 sr, and the ratio ρ_p/ρ_H is approximately .85 for these measuring spheres. A discussion of some common causes for measurement errors of this type is given in appendix F and ways to estimate values for ε_p and ε_r are given for each cause. The magnitude of ε_p and ε_r is usually quite small, except when samples of different surface textures are compared using the 0° incidence sphere, in which case ε_p can be quite large. For this reason the 6° incidence sphere will usually be used for directional-hemispherical measurements with this instrument.

e. Sample plane to port plane displacement effect

The general purpose measuring sphere with 6° incident angle (specular component included) was tested for sample plane to port plane distance effect on the relative reflectance measurement. A $BaSO_4$ sample was measured from 400 nm to 750 nm with four sample locations: the sample plane 0.9 mm into the measuring sphere from the normal location, at the normal location, and 0.9 mm and 1.8 mm out of the measuring sphere from its normal location. The differences of the relative reflectance from that in the normal position were 0.0009, 0, -0.0019, and -0.0054 respectively. Since the sample surface can be prepared and mounted within 0.1 mm to the port, the uncertainty in the relative reflectance measurement will be less than 0.0002.

B. Integrating Sphere for Measuring Relative Directional-Hemispherical Reflectance as a Function of Angle of Incidence

1. Description

The integrating sphere used in the measurement of relative directional-hemispherical reflectance as a function of angle of incidence is illustrated in figure 8. This 45 cm diameter sphere is mounted on a kinematic support system for ease of alignment when this device is to be used with the spectrophotometer system. The sphere is designed so that a sample can be suspended in the center of the sphere where it intercepts the sample beam. The sample surface is at the sphere center and the sample can be rotated 360° about the sphere center by means of a stepping motor controlled turntable at the top of the sphere. The turntable and the support rod on which the sample is mounted can be removed as a unit for changing samples. The beam goes through a cylindrical lens with its focal line at the center of the sphere and then enters the sphere through an aperture just large enough to allow its entry. A removable plug opposite the sample beam entry port, is opened to initially align the beam through the center of the sphere. To determine the correct position of the turntable for intercepting the beam at normal to the sample, a mirror is suspended in the center of the sphere and rotated until the beam reflects back out the entrance port. The mirror is then replaced with the sample to be measured. The stepping motor is programmed to turn the sample to any desired angle of incidence in the clockwise and counterclockwise direction.

The multiplier phototude detector is located in the bottom of the sphere. The diffuse radiation from the sphere must pass through the side of a transparent plastic rod projecting

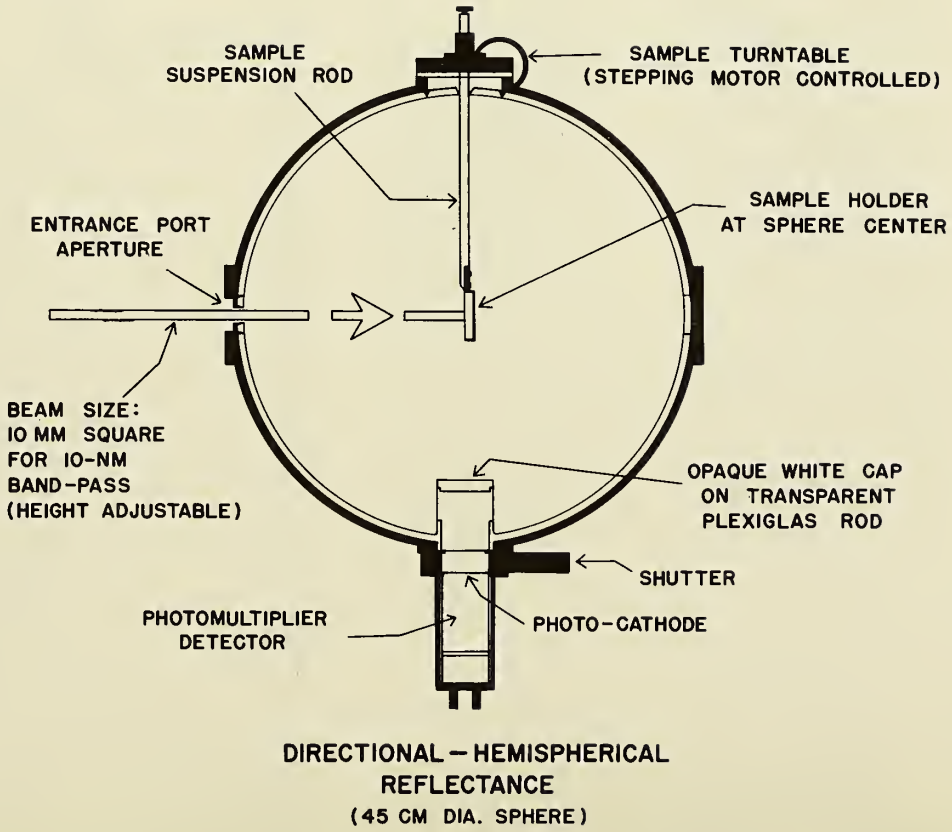

Figure 8. Integrating sphere for measuring relative directional-hemispherical reflectance as a function of angle of incidence.

into the sphere above the detector, in order to be measured. The top of this rod is capped by an opaque white coating and the lower portion of the rod is enclosed in the same white material as the sphere coating. These two coatings act as baffles to prevent direct reflections from the sample to the detector. The plastic rod acts as a light pipe in transmitting the signal to the detector and also acts as a rotationally symmetric support for the upper baffle. A shutter is provided to protect the detector when the room lights are turned on. The sphere coating is tetrafluorethylene powder, which completely seals the seam where the two hemispheres are joined during assembly.

2. Measurement Procedure

With the sample mounted in the center of the sphere and with only the sample beam in use the relative directional-hemispherical reflectance of the sample at angle of incidence of θ to that at normal incidence was determined using the following procedure. We choose to record data in the order of Z, N_0, $N_{+\theta}$, $N_{-\theta}$, $N_{-\theta}$, $N_{+\theta}$, N_0, Z and corresponding times t_1, t_2, t_3, t_4, t_6, t_7, t_8, t_9. The time which occurred about half way between two $N_{-\theta}$'s was also recorded as t_5. N_0 is the signal at normal incidence; $N_{+\theta}$ and $N_{-\theta}$ are signals with angle of incidence of θ at opposite sides of the normal; and Z is the dark current reading. A computer program was written to analyze the data in the following manner. The signals of Z, N_0, $N_{+\theta}$, and $N_{-\theta}$ are first linearly interpolated in time to obtain a value for each at time t_5. The ratio Q_θ of the uncorrected relative directional hemispherical reflectance of the sample at angle of incidence of θ to that at normal incidence is then computed as

$$Q_\theta = \frac{Q_{\theta/h}}{Q_{0/h}} = \frac{[N_{+\theta}(t_5) - Z(t_5)] + [N_{-\theta}(t_5) - Z(t_5)]}{2[N_0(t_5) - Z(t_5)]} \qquad (12)$$

The procedure above is carried out for polarizations parallel and perpendicular to the plane of incidence and the results are averaged.

Computer programs for the control system have been written which scan the wavelength to obtain the spectral relative directional-hemispherical reflectance of the sample at one angle of incidence and which scan the angle of incidence at any desired interval at a fixed wavelength to obtain the goniometric relative directional-hemispherical reflectance of the sample at one wavelength.

3. The Entrance Port Correction

Some of the radiation reflected from the sample is lost out the entrance port. The amount of radiation lost depends upon the angle of incidence because of the cosine law and it may be affected further by non-Lambertian angular distribution of the reflected radiance. To make the principal correction for this, we assume that the sample is a Lambertian reflector. The fraction, f, of the reflected flux which escapes through the entrance port from the sample when it is at normal incidence is

$$f = \frac{A/R^2}{\pi} \qquad (13)$$

where A is the effective non-reflecting area of the entrance port, R is the inner radius of the integrating sphere, and π is the projected solid angle of the entire hemisphere. For other angles of incidence θ, the fraction of the reflected flux which escapes through the entrance port from the sample is f $\cos\theta$.

The ratio Q_θ, can be expressed by the true directional-hemispherical reflectance $\rho_{\theta/h}$ at angle θ and $\rho_{0/h}$ at normal as

$$Q_\theta = \frac{Q_{\theta/h}}{Q_{0/h}} = \frac{\rho_{\theta/h}(1 - f\cos\theta)}{\rho_{0/h}(1 - f)} \qquad (14)$$

Solving for the ratio q_θ of $\rho_{\theta/h}$ to $\rho_{0/h}$, we have

$$q_\theta = \frac{\rho_{\theta/h}}{\rho_{0/h}} = Q_\theta \frac{1 - f}{1 - f\cos\theta} \qquad (15)$$

C. Auxiliary Spheres for Determination of the Absolute Reflectance Scale

The general purpose integrating sphere illustrated in figure 5, is equipped with a sample flange for mounting an auxiliary sphere as shown in figure 9. The theory of the use of this type of sphere to determine the absolute reflectance of a material has been described in earlier papers [10,11]. Three of these auxiliary spheres have been constructed having diameters of 30 cm, 20 cm, and 15 cm. The sphere illustrated in figure 9 is the 30 cm diameter auxiliary sphere, which is the same diameter as the detector sphere. These spheres are used to determine the absolute reflectance of white coatings applied to the auxiliary sphere. They have removable target plates that can be attached directly to the detector sphere. These spheres have entrance apertures 2.54 cm in diameter and the removable target is a section of the sphere of 5.08 cm diameter. The spheres are designed to allow the inside curvature of the white coating to meet the center of the entrance port. The edge of the entrance port is beveled about 30° on the side facing the detector sphere, thus providing a clean knife edge for the port. The sample beam enters the auxiliary sphere and is incident on the target at 6° from normal to allow any specular component to be included in the integration of the signal in this sphere. The coatings are applied to the two hemispheres which can be attached to each other so as to completely seal the seam between the hemispheres.

Details of the use of these auxiliary spheres to determine directional-hemispherical reflectance factor are to be given in a separate publication.

D. Bidirectional Diffuse Reflectance and Transmittance Factor Accessory System

A system has been constructed for utilizing the diffuse reflectance spectrophotometer in measuring bidirectional reflectance factor, particularly for 45°-0°. With this accessory set up for 45°-0° as shown in figure 10, the collimated sample beam from the spectrophotometer is incident on a sample at 45° from normal and the reflected signal at normal to the sample is collected and measured. The multiplier phototube detector is equipped with a signal averaging sphere. The detector and averaging sphere are attached to a stepping motor controlled vertical slide for alignment and scanning purposes. The averaging sphere has a limiting aperture facing the sample. The solid angle of collection is determined by the size of the limiting aperture and its distance from the sample. In this system the sample is mounted on a stepping motor controlled turntable, and the detector assembly is on an arm attached to another independently controlled turntable having the same axis of rotation as the sample turntable.

The sample is mounted on a two position slide that moves 12.5 cm between positions and is pneumatically driven. In one position the sample intercepts the beam, in the second position a polished black glass standard intercepts the beam. The polished black glass is mounted so that it intercepts the beam at 22.5° from its normal and the specular reflection, amounting to approximately 4%, is reflected into the detector averaging sphere. This black glass acts as a standard reflector. It has a specular signal level of about 40 times the magnitude of the diffuse signals that will be measured. Alignment is accomplished with the alignment laser built into the spectrophotometer. The stepping motors are controlled by computer to allow for scanning the detector position or changing the incident angle on the sample or viewing angle from the sample. This device has not been tested at the date of this publication.

IV. SUMMARY

Because of the modular nature of this instrument, it will probably never be completed in the sense that no more accessories will be constructed. Therefore it was decided to publish this technical note to document the development and testing of the NBS Reference Spectrophotometer for Diffuse Transmittance and Reflectance from its inception to the present (May 1976). The principal use of the instrument to date has been to investigate problems connected with realizing a scale of directional-hemispherical reflectance factor. The results of this investigation are to be published separately.

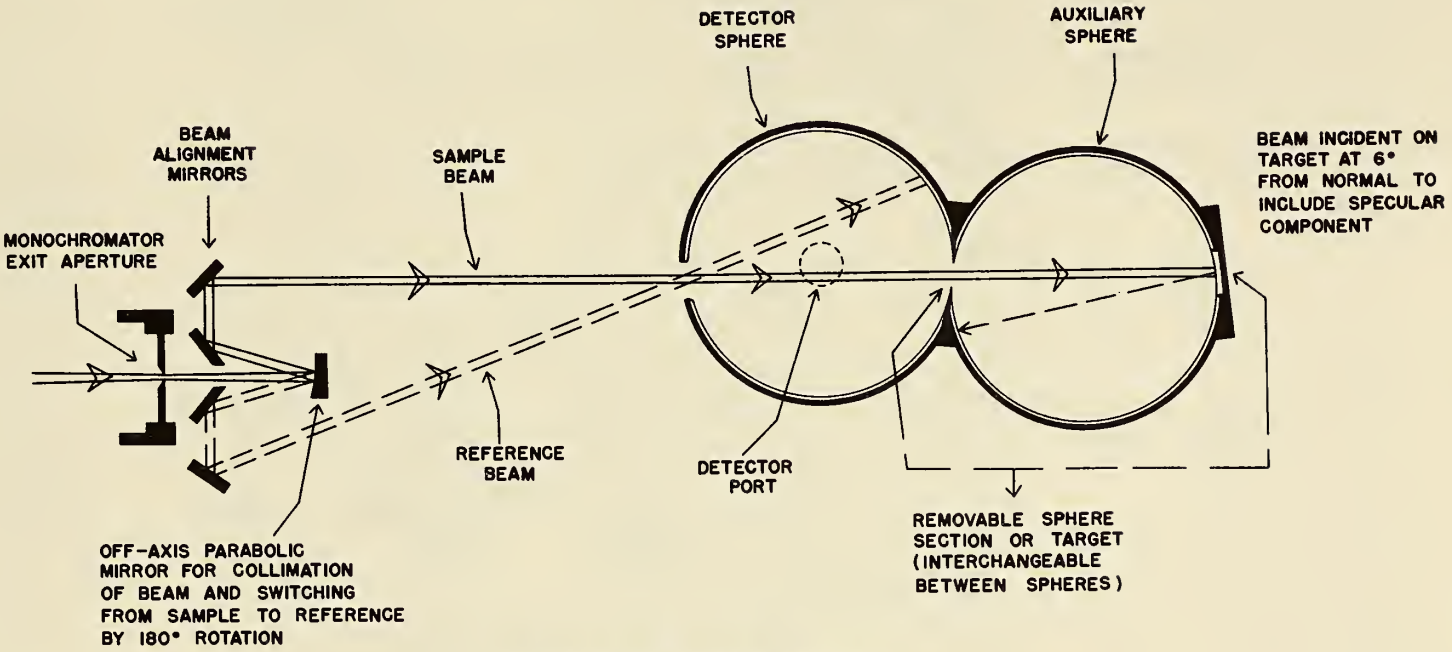

Figure 9. The auxiliary sphere system for determination of an absolute reflectance scale.

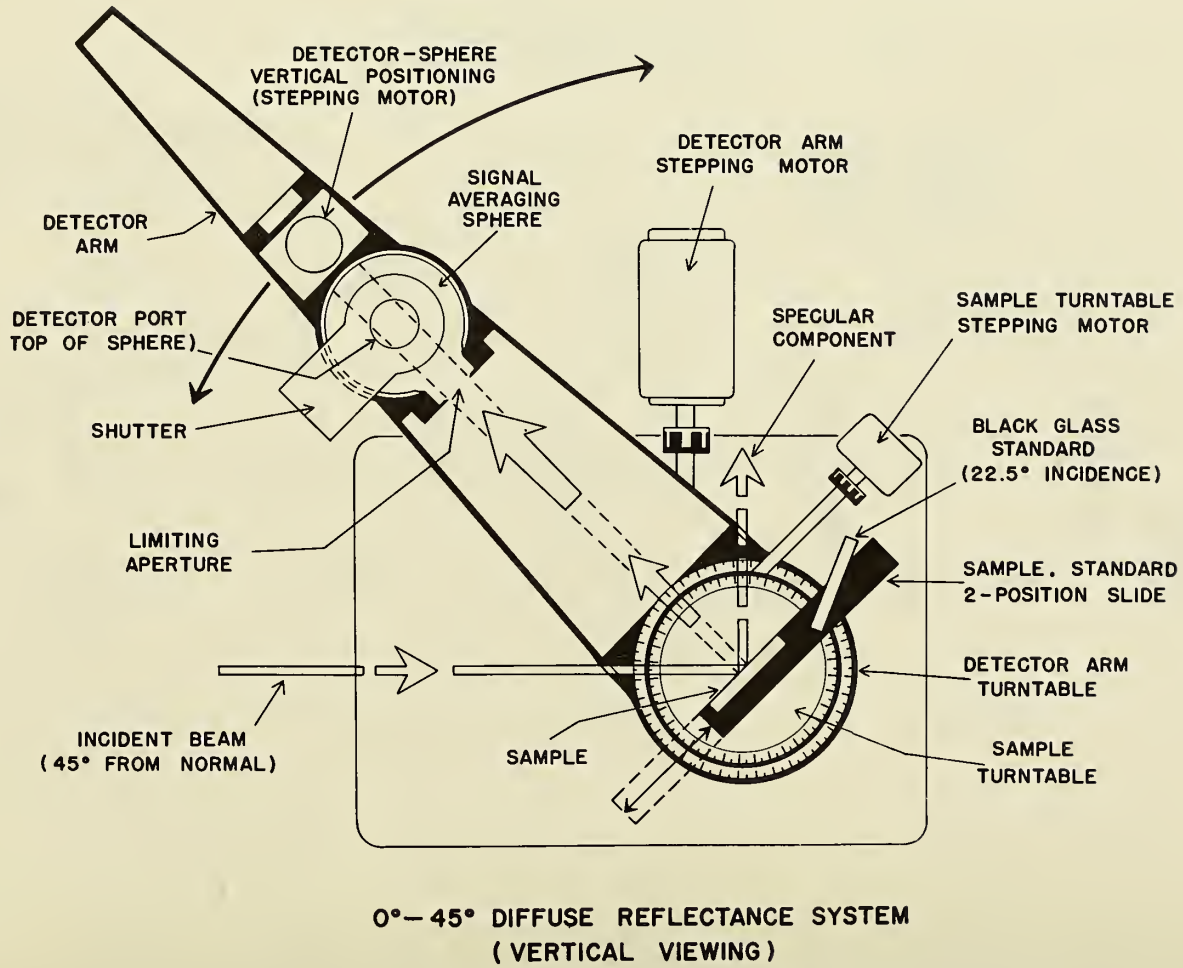

Figure 10. Bidirectional reflectance factor system.

APPENDIX A

Sample-Induced Nonlinearity

The type of nonlinearity to be discussed here is not the result of detector or electronic nonlinearity, but is the result of slight differences in the efficiency with which the radiation reflected from the sample and the radiation from the reference beam, reflected from the wall, reaches the detector. Since the sample when presented at the sample port becomes part of the sphere wall, it affects the efficiency of the sphere in transmitting the radiation from the initial reflection of the sample beam or of the reference beam to the detector. In an ideal situation in which the sample is curved to fit the contour of the sphere wall and all reflections are Lambertian, the efficiency for transmitting radiation from the initial reflection from either beam will be the same, so that

$$Q_x = \frac{\phi_1 \rho_x}{\phi_2 \rho_w} \tag{A1}$$

where Q_x is the relative reflectance as defined in eq. (2), ϕ_1 is the flux incident upon the sample, ρ_x is the directional-hemispherical reflectance of the sample x, ϕ_2 is the flux incident upon the sphere wall, and ρ_w is the directional-hemispherical reflectance of the sphere wall. However, real spheres seldom operate under such ideal conditions, so that a more complex and non-linear relationship exists between Q_x and ρ_x. Because this departure from linearity is small, it can usually be adequately represented by adding a small quadratic term in ρ_x to the right side of eq. (A1).

Three cases of such nonlinearity will be discussed in the remainder of this appendix. In each case, the following approach will be taken in the analysis. The reflected flux from the initial reflection of each beam will be described in terms of two or more parts. The principal part of each flux will be that part which can reasonably be expected to reach the detector with the same efficiency from both beams. The remaining parts of the flux will be transferred with different efficiencies and will be the cause of the non-linearity. Since the component which receives the same treatment will be by far the largest, the contribution of the detected flux from each reflection of the other fluxes can be written in terms of a rapidly converging geometric series. The sum of such a series can be evaluated and eventually written in an approximate simple quadratic form.

1. Wall Retro-Reflectance Nonlinearity

If the sphere wall coating retro-reflects, a simple model of the reflection from the sphere wall is one in which a fraction f_0 of the incident radiation is returned in precisely the opposite direction to the direction of incidence and the remaining fraction $(1-f_0)$ is reflected diffusely with a Lambertian distribution and will be transmitted to the detector through the sphere with an efficiency η_x. The retroreflected portion will be returned to the sample, where it will again be reflected with a reflectance ρ_x. (In discussing the reflectance from the sample, the sample will be treated as being non-retroreflecting, since the initial retroreflective component, if any, will be lost out the entrance port and the remaining contribution will produce only a small change in an already small correction term.) Thus, the signal* from the first reflection from the sphere wall will be:

$$N_{x1} = \phi_1 \rho_x (1 - f_0)\, \eta_x \tag{A2}$$

where ϕ_1 is the flux in the beam of radiation incident on the sample. Let f' be the fraction of the reflected radiation which strikes the sphere wall as opposed, for example, to going out the ports. It is assumed here that the sphere contains a baffle which prevents radiation reflected from the sample from going directly to the detector. The retroreflected fraction

---

*In these appendices, the signal being discussed is the signal above background. In terms of the notation in section III.A.2, $N_x = N'_x - Z$ where N'_x is corrected for any detection system nonlinearity.

returns to the sample and is reflected again. Of the re-reflected radiation, a fraction $(1-f_0)$ makes a second contribution to the signal;

$$N_{x2} = \phi_1 \rho_x [f_0 \bar{\rho}_x f'](1 - f_0)\, \eta_x. \tag{A3}$$

where $\bar{\rho}_x$ is the reflectance of the sample for hemispherically incident radiation. Similar expressions can be written for the remaining contributions. The contributions form a geometric series in which the initial term is N_{x1} and the ratio of successive terms is the factor in brackets in eq. (A3). The entire signal is, then, the sum of the series, or:

$$N_x = \frac{\phi_1 \rho_x (1 - f_0)\, \eta_x}{1 - f_0 \bar{\rho}_x f'} \tag{A4}$$

When the signal from the reference beam is treated in the same way, a similar expression, in which ρ_x is replaced by ρ_w, ϕ_1 is replaced by ϕ_2, and $\bar{\rho}_x$ is replaced by $\bar{\rho}_w$ will result. The ratio of these two signals will be Q'_x, so that

$$Q'_x = \frac{\phi_1 \rho_x}{\phi_2 \rho_w} A_2 (1 + G_2 \bar{\rho}_x) \tag{A5}$$

where

$$A_2 = (1 - G_2 \bar{\rho}_w)$$

and

$$G_2 = f_0 f'$$

and terms in higher powers of $G_2 \bar{\rho}_x$ have been dropped. It can be seen that (A5) has the form of (A1) with a corrective term which depends upon the reflectance $\bar{\rho}_x$ of the sample. In reality, the retro-reflected radiation is not returned from the wall in exactly the direction it arrives, but is spread out typically in a distribution with a half-height width of a degree or two. However, in the usual case in which the initial radiation is reflected from the center of the sample, most of the retroreflected radiation is returned to some point on the sample, so that f_0 probably represents most of the radiation in the retroreflective peak along with a less easily defined contribution (either positive or negative) due to the fact that the level of the underlying diffuse radiation in the retro direction may be above or below the average of the distribution. Because of this difficulty in defining f_0 precisely, it is best evaluated using experiments such as are described in appendix B.

2. Flat-Sample Nonlinearity

As is indicated in the literature [12], if the sample is flat, the comparison between sample and reference may not be exact. The nonlinearity in this case arises because the sample does not reflect directly onto itself, whereas if the sphere design is such that the reference beam strikes the sphere at a point on the curved wall, some of the radiation from the first reflection does strike the sample. The signal due to the radiation reflected from the sample is given by

$$N_x = \phi_1 \rho_x \eta_x \tag{A6}$$

where η_x is the average efficiency of transfer to the detector for radiation striking the sphere wall anywhere outside the sample port. If the sample port receives a fraction f_1 of the radiation from the initial reflection of the reference beam, the signal from the reference beam is given approximately by

$$N_w = \phi_2 \rho_w [(1 - f_1) + f_1 \rho'_x] \eta_x \quad \text{(A7)}$$

where ρ'_x is the reflectance of the sample for radiation incident on it from the direction of the point of incidence of the reference beam. In this case, the ratio Q'_x becomes

$$Q'_x = \frac{\phi_1 \rho_x}{\phi_2 \rho_w} A_1 (1 + G_1 \rho'_x) \quad \text{(A8)}$$

where

$$A_1 = 1/(1 - f_1)$$

and

$$G_1 = -f_1/(1 - f_1)$$

Note that in this case, the nonlinearity term is of the opposite sign from the retroreflective term so that the two contributions will tend to cancel.

3. Baffle-Induced Nonlinearity

In principle, the flat-sample nonlinearity just discussed can be avoided by placing the sample port and the surface struck by the reference beam in the same plane in the way that was done by Hardy [13]. However, this distorts the sphere considerably, so we chose to reduce the flat sample nonlinearity by introducing a small baffle between the sample port and the point of incidence of the reference beam. A sphere with baffle is shown in cross section in figure 11. Because of the presence of the baffle, the analysis becomes quite complex and depends upon the design of the baffle and the choice of the point of incidence of the reference beam. This analysis will be carried out in detail in appendix E to evaluate the specific sphere design we used. However, the procedure for carrying out the analysis and the nature of the results can be discussed in general. The reflecting areas in the sphere are divided up into six regions: region 1, the sample port; region 2, the portion of the sphere wall struck directly by the radiation reflected from the sample but not struck by the radiation reflected directly from the area irradiated by the reference beam; region 3, the side of the baffle toward the sample port; region 4, the side of the baffle away from the sample port; region 5, the portion of the sphere wall which is struck by the radiation from the initial reflection of the reference beam, but which is not struck by radiation reflected from the sample; and region 6, the remaining portion of the sphere. In a good sphere design of this type, region 6 is by far the largest region and it contains the detector port. In the analysis, once the radiation reaches region 6, it is assumed to be transferred to the detector with an efficiency η_x which is independent of the beam from which the radiation originated.

Although the solution of the problem of the transfer of the radiation from the point of incidence of the sample beam to region 6 is difficult, the form of the result can be anticipated.

$$N_x = \phi_1 \rho_x (a_x + b_x \rho'_x) \eta_x \quad \text{(A9)}$$

where a_x and b_x are independent of the sample and depend only on the sphere geometry and the wall and baffle reflectances. The constant a_x is nearly 1 and represents the portion of the radiation which reaches region 6 without additional reflections from the sample, b_x represents the portion of the radiation which is reflected again by the sample before reaching region 6, and ρ'_x is the effective reflectance of the sample for irradiation from regions 2, 3 and 5. A similar expression can be written for the reference beam

$$N_w = \phi_2 \rho_w (a_w + b_w \rho'_x) \eta_x \quad \text{(A10)}$$

where a_w, also nearly 1, represents the portion of the radiation transferred to region 6 without reflecting from the sample and b_w represents the portion reaching region 6 by reflecting from the sample. The signal ratio Q'_x takes the same form as in eq. (A8), except in this case

$$A_1 = \frac{a_x}{a_w}$$

and

$$G_1 = \left(\frac{b_x}{a_x} - \frac{b_w}{a_w} \right) \quad \text{(A11)}$$

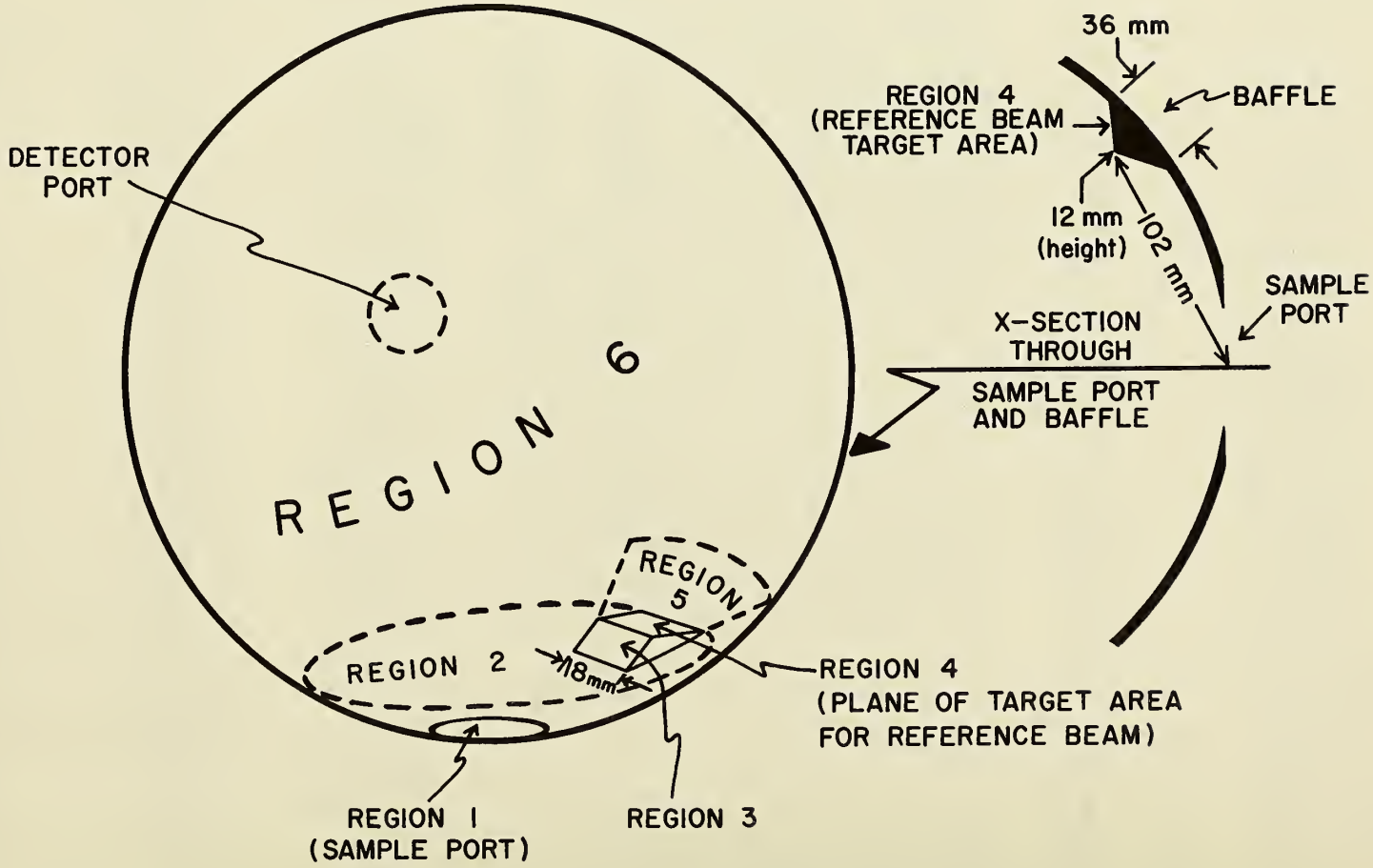

Figure 11. Pictorial representation of the sphere with baffle. The baffle is a triangular wedge built up with sphere wall material, and the reference beam is incident upon the wall of the baffle which is away from the sample port.

Because of the baffle's shielding effect, $b_x > b_w$ so that in this case G_1 is positive and the baffle-induced nonlinearity tends to be of the same sign as the wall retro-reflectance nonlinearity.

4. Combinations of Sample-Induced Nonlinearities

If the sample-induced nonlinearities are small, the wall retro-reflective nonlinearity term can simply be added to the appropriate geometrically-related nonlinearity term to yield an expression of the form:

$$Q'_x = \frac{\phi_1}{\phi_2} \frac{\rho_x}{\rho_w} A_1 A_2 (1 + G_1 \rho'_x + G_2 \bar{\rho}_x) \qquad \text{(A12)}$$

where G_1 is given either by eq. (A8) or eq. (A11), depending upon the absence or presence of a baffle, and where G_2 is given by eq. (A5). Because of the sample-induced nonlinearities, it follows that the ratio of the actual reflectances of two samples y and x can be obtained from correcting the ratio of the corresponding measured values Q_y and Q_x. This correction can be determined from eq. (A12) to be:

$$\frac{\rho_y}{\rho_x} = \frac{Q'_y}{Q'_x} [1 + G_1(\rho'_x - \rho'_y) + G_2(\bar{\rho}_x - \bar{\rho}_y)] \quad . \qquad \text{(A13)}$$

APPENDIX B

Method of Evaluating Sample-Induced Nonlinearity

The sample-induced nonlinearity can be evaluated by using two thin masks, each of which has a hole in it. The masks are identical in size, but one is painted black and the other is painted white. The hole in the mask is made smaller than the sample port, but larger than the irradiated area on the sample. Two measurements are made on a given sample, one with each mask in place between the sample and the sphere port. In both of these measurements, the relative reflectance must be corrected for scattered radiation surrounding the main incident beam as discussed in appendix C. For each measurement, the mask is aligned so that the incident beam passes through the hole. In this way, the average reflectance of what appears in the sample port can be changed without changing the surface which is initially struck by the incoming beam of radiation. Equation (A13) can be modified to give the measured relative reflectance with the white mask in place as:

$$Q'_{xA} = \frac{\phi_1 \rho_x}{\phi_2 \rho_w} A_1 A_2 \left\{ 1 + G_1[(1-F_1)\,\rho'_x + F_1 \rho'_A] + G_2[(1-F_2)\bar{\rho}_x + F_2 \bar{\rho}_A] \right\} \tag{B1}$$

where F_1 is the ratio of the area of the mask to the area of the sample port, F_2 represents the fraction of the retroreflected radiation which spills over from the irradiated area of the sample onto the mask, during the interreflections, ρ'_A is the reflectance of the white mask at the same angle of incidence at which ρ'_x is evaluated and $\bar{\rho}_A$ bears a similar relation to $\bar{\rho}_x$. (See discussion proceeding eq. (A8) and following eq. (A3) in appendix A.) It is expected that F_2 will be smaller than F_1.

A similar equation can be written for the black mask to obtain a relative reflectance Q'_{xB}. Taking the ratio Q'_{xB} to Q'_{xA} one obtains

$$1 - \frac{Q'_{xB}}{Q'_{xA}} = G_1 F_1 (\rho'_A - \rho'_B) + G_2 F_2 (\bar{\rho}_A - \bar{\rho}_B) \tag{B2}$$

where use is made of the assumption that $G_1 << 1$ and $G_2 << 1$. Since the correction coefficients G_1 and G_2 are small, there will be a large uncertainty in determining them. Therefore, the approximations used to determine the correction term in eq. (8) will be made conservatively, i.e., in such a way as to make the correction small in order to avoid overcorrection. The relative reflectance Q'_A and Q'_B of the mask materials can be measured. Since $\phi_1 \simeq \phi_2$ and $\rho_w \simeq 1$, these measured values can be used in place of ρ'_A and $\bar{\rho}_A$ in the first term of eq. (B2) and also in place of ρ'_B and $\bar{\rho}_B$ in the second term of eq. (B2). With this assumption, eq. (B2) can be written

$$\frac{1 - Q'_{xB}/Q'_{xA}}{F_1(Q'_A - Q'_B)} = G_1 + \frac{F_2}{F_1} G_2 \equiv \alpha \tag{B3}$$

Under the same assumption, eq. (A13) can be written as

$$\frac{\rho_y}{\rho_x} = \frac{Q'_y}{Q'_x}\left[1 + (G_1 + G_2)(Q'_x - Q'_y)\right] \tag{B4}$$

Since $F_2 < F_1$, it follows that

$$|\alpha| \leq |G_1 + G_2| \tag{B5}$$

when G_1 and G_2 have the same sign. Therefore, in the case of the sphere with baffle, eq. (8) provides a conservative correction when α is determined using eq. (B3).

APPENDIX C

Correcting for Scattered Radiation in Incident Beam

The beam of radiation incident on the sample can be considered to be made up of three fluxes: ϕ_1, which falls inside a given central circle and contains most of the incident radiation, ϕ_b which falls between the central circle and the boundary of the sample port, and ϕ_c which falls outside the boundary of the sample port. These three make up the total incident flux ϕ_{xmw}, i.e.

$$\phi_{xmw} = \phi_1 + \phi_b + \phi_c \tag{C1}$$

where $\phi_1 >> \phi_b$ and $\phi_1 >> \phi_c$ is the case in a good instrument. An expression for the uncorrected relative reflectance Q''_x as read from the instrument is

$$Q''_x = k\phi_1\rho_x\{1 + G_1[(1 - F_1)\,\rho'_x + F_1\rho'_m] + G_2[(1 - F_2)\,\rho_x + F_2\rho_m]\} + k\phi_b\rho_m + k\phi_c\rho_w \tag{C2}$$

where ρ_x is the reflectance of the sample in the central area, ρ_m is the reflectance of the sample in the area struck by ϕ_b, F_1 and F_2 are defined after eq. (B2) and, products of two small terms are neglected, and k is $A_1A_2/\phi_2\rho_w$. (See discussion in last paragraphs of appendix A.) One would like to correct Q''_x to obtain the contribution due just to the light reflected from the central area, i.e.

$$Q'_x = k\phi_1\rho_x\{1 + G_1[(1 - F_1)\,\rho'_x + F_1\rho'_m] + G_2[(1 - F_2)\,\rho_x + F_2\rho_m]\} \tag{C3}$$

To make this correction, four additional measurements are made. First a value of Q''_x is obtained with the sample port empty. This is called Q''_w and is given by:

$$Q''_w = k\phi_c\rho_w \tag{C4}$$

Second the value of Q''_x is obtained with a white card in the area struck by ϕ_b and the central area empty (a hole in the card). This is called Q''_{cw} and is given by:

$$Q''_{cw} = k(\phi_b\rho_c + \phi_c\rho_w) \tag{C5}$$

where ρ_c is the reflectance of the card. Third a value of Q''_x is obtained with a white card of the same material filling the entire port. This is called Q''_{ccw} and is given by:

$$Q''_{ccw} = k\phi_1\rho_c(1 + G_1\rho'_c + G_2\rho_c) + k\phi_b\rho_c + k\phi_c\rho_w \tag{C6}$$

For measurements in which the area struck by ϕ_b is to be occupied by a mask of reflectance ρ_m, a measurement of Q''_x with only the mask in place can be made. This is called Q''_{mw} and is given by:

$$Q''_{mw} = k(\phi_b\rho_m + \phi_c\rho_w) \tag{C7}$$

when a mask is used, a correction of the general measurement can be made as:

$$Q'_x = Q''_x - Q''_{mw} \tag{C8}$$

This expression is used to obtain Q'_{xA} and Q'_{xB} in appendix B. When the entire sample port is filled with the same material ($\rho_m = \rho_x$), one can correct Q''_x to give Q'_x as shown in eq. (C3) by using

$$Q'_x = (Q''_x - Q''_w)\,\frac{(Q''_{ccw} - Q''_{cw})}{(Q''_{ccw} - Q''_w)} \tag{C9}$$

This expression is used when comparing a sample without mask to a sample with mask for which eq. (C8) applies. This circumstance occurs in the use of the auxiliary sphere attachment described in III.C.

When two samples are to be compared, each of which fills the entire entrance port, a simpler correction is applicable. In this case, the mask area and, therefore ϕ_b, is considered to be zero and the corrected relative reflectance is:

$$Q'_x = k\phi_1\rho_x(1 + G_1\rho'_x + G_2\bar{\rho}_x) \tag{C10}$$

This can be obtained from the uncorrected values as:

$$Q'_x = Q''_x - Q''_w \tag{C11}$$

APPENDIX D

Test for Polarization Effects

The incident radiation can be polarized using a polarizer in the input optics as indicated in figure 2. The monochromator will not depolarize the radiation if the plane of polarization is either perpendicular to or parallel to the plane of the monochromator. For the polarization tests, the instrument is used in a single-beam mode, and the measurements are made in a time-symmetrical sequence to allow correction for linear drift of the source and detector in time.

To determine whether the reflectance measurement on a sample is polarization dependent, the ratio of the fluxes $\phi_{/\!/}$ and $\phi_{\perp}$ with the beam in the two polarizations is determined by using a second integrating sphere as a target. This sphere acts as a polarization insensitive target which effectively reflects depolarized radiation. The ratio q_a of the signals, equal to the ratio of the incident fluxes in this case, is

$$q_a = \frac{\phi_{/\!/}}{\phi_{\perp}} \tag{D1}$$

If a highly polarizing diffusing reflector is measured with $\phi_{/\!/}$ incident and then rotated 90° and measured with $\phi_{\perp}$ incident, the ratio q_b is determined.

$$q_b = \frac{\eta_{/\!/}\,\phi_{/\!/}}{\eta_{\perp}\,\phi_{\perp}} \tag{D2}$$

where $\eta_{/\!/}$ and $\eta_{\perp}$ are the sample beam efficiencies of the sphere for the given polarization. The polarizing diffuse reflector is made by cementing an absorbing polarizing film on a piece of white opal glass and using it in the orientation for maximum reflectance of the polarized light. If q_a and q_b are equal, the measuring sphere is polarization independent.

Finally, the polarization dependence of a sample can be evaluated by obtaining signals for each polarization to determine the ratio q_c.

$$q_c = \frac{\rho_{/\!/}\,\eta_{/\!/}\,\phi_{/\!/}}{\rho_{\perp}\,\eta_{\perp}\,\phi_{\perp}} \tag{D3}$$

where $\rho_{/\!/}$ and $\rho_{\perp}$ are the sample reflectances for the two polarizations with the given orientation of the sample. If $q_b = q_c$, the sample reflectance is polarization independent.

APPENDIX E

Estimation of Sample-Dependent Nonlinearity

In this appendix, an approximate evaluation of the constants G_1 defined in appendix A will be made for the general purpose integrating sphere. The measured dimensions of the spheres will be used as a basis for the estimation. The radius of the interior wall of the sphere is R = 14.6 cm and the sample port takes the form of a circle of radius r = 2.54 cm on this surface.

1. Sphere Without Baffle

From elementary geometry and the assumption of Lambertian reflection from the sphere wall, the fraction f_1 of the radiation reflected from the reference beam into the sample is

$$f_1 = 1/2\left[1 - \sqrt{1 - \frac{r^2}{R^2}}\right] \tag{E1}$$

Thus one can evaluate G_1 for this sphere from eq. (A8) as

$$G_1 = 0.0077$$

2. Sphere With Baffle

The treatment of a sphere with a baffle is considerably more complicated and a method of detailed flux balance will be used here to obtain an estimate of G_1 as given in eq. (A11). The flux ϕ_{nm} transferred from region n to region m can be obtained from evaluating an expression of the following form:

$$\phi_{nm} = \iint \frac{L_n \cos\theta_n \cos\theta_m \, dA_n \, dA_m}{D^2} \tag{E2}$$

where L_n is the radiance leaving dA_n, dA_i is an element of area on surface i, (i = m or n), D is the length of the line connecting dA_n to dA_m, and θ_i is the angle between the connecting line and the normal to dA_i. In the present estimate, this expression will be approximated as:

$$\phi_{nm} = L_n \, V_{nm} \tag{E3}$$

where the quantities V_{nm} are given by

$$V_{nm} = \iint \frac{\cos\theta_n \cos\theta_m \, dA_n \, dA_m}{D^2} \tag{E4}$$

The assumption here is that L_n is uniform at some average value over the entire region n. Except for the case when regions n and m are both on the sphere and in clear view of each other, it is difficult to evaluate V_{nm} exactly. For the general purpose integrating sphere described in section III and pictured in figure 11, rough estimates were made of the areas A_n of each region and the non-zero V_{nm}. (A V_{nm} would be zero if no part of region m is visible from region n.) The areas A_n were first determined, and then approximate V_{nm} not involving area 6 were obtained from the geometry of the sphere and baffle. The sum of all the V_{nm} involving region n must be

$$\sum_{m=1}^{6} V_{nm} = \pi A_n \tag{E5}$$

From which V_{n6} is calculated as

$$V_{n6} = \pi A_n - \sum_{m=1}^{5} V_{nm} . \qquad \text{(E6)}$$

This, with the fact that $V_{nm} = V_{mn}$, assures that the set of V_{nm} and A_n are consistent, even if only approximate. These values are presented below with the numbering of the regions the same as described in the first paragraph of part 3 in appendix A and as illustrated in figure 11.

A_n (cm^2)

$A_1 = 20.3$	$A_4 = 3.9$
$A_2 = 299$	$A_5 = 3.5$
$A_3 = 3.9$	$A_6 = 2350$

V_{nm} (cm^2 - steradian)

$V_{12} = 7.1$	$V_{26} = 821$
$V_{13} = 0.28$	$V_{36} = 6.7$
$V_{16} = 56$	$V_{45} = .55$
$V_{22} = 105$	$V_{46} = 12$
$V_{23} = 5.3$	$V_{55} = 0.014$
$V_{25} = 0.7$	$V_{56} = 9.6$

Figure 12 is a schematic illustration of the radiation transfer in the sphere. If the radiation is considered to be detected once it reaches the "common ground", region 6, then the fact that it is afterwards reflected and re-reflected need not be considered further and flux balancing equations can be set up which deal with only the photons which have never reached region 6. If L_{xn} is the radiance L_n leaving the surface of region n when the sample x is irradiated by the incoming beam, the following set of flux balance equations can be set up with the aid of figure 12.

$$\pi A_1 L_{x1} = \phi_1 \rho_x + (V_{12} L_{x2} + V_{13} L_{x3})\, \rho'_x \qquad \text{(E7)}$$

$$\pi A_2 L_{x2} = (V_{12} L_{x1} + V_{22} L_{x2} + V_{23} L_{x3} + V_{25} L_{x5})\, \rho_w \qquad \text{(E8)}$$

$$\pi A_3 L_{x3} = (V_{13} L_{x1} + V_{23} L_{x2})\, \rho_w \qquad \text{(E9)}$$

$$\pi A_4 L_{x4} = (V_{45} L_{x5})\, \rho_w \qquad \text{(E10)}$$

$$\pi A_5 L_{x5} = (V_{25} L_{x2} + V_{45} L_{x4} + V_{55} L_{x5})\, \rho_w \qquad \text{(E11)}$$

Using the A_n and the V_{nm} from the foregoing list, the radiances L_{xn} can be determined by simultaneous solution of these equations in terms of ϕ_1 ρ_x ρ'_x and ρ_w. From these, the signal N_x corresponding to the sample beam can be calculated as:

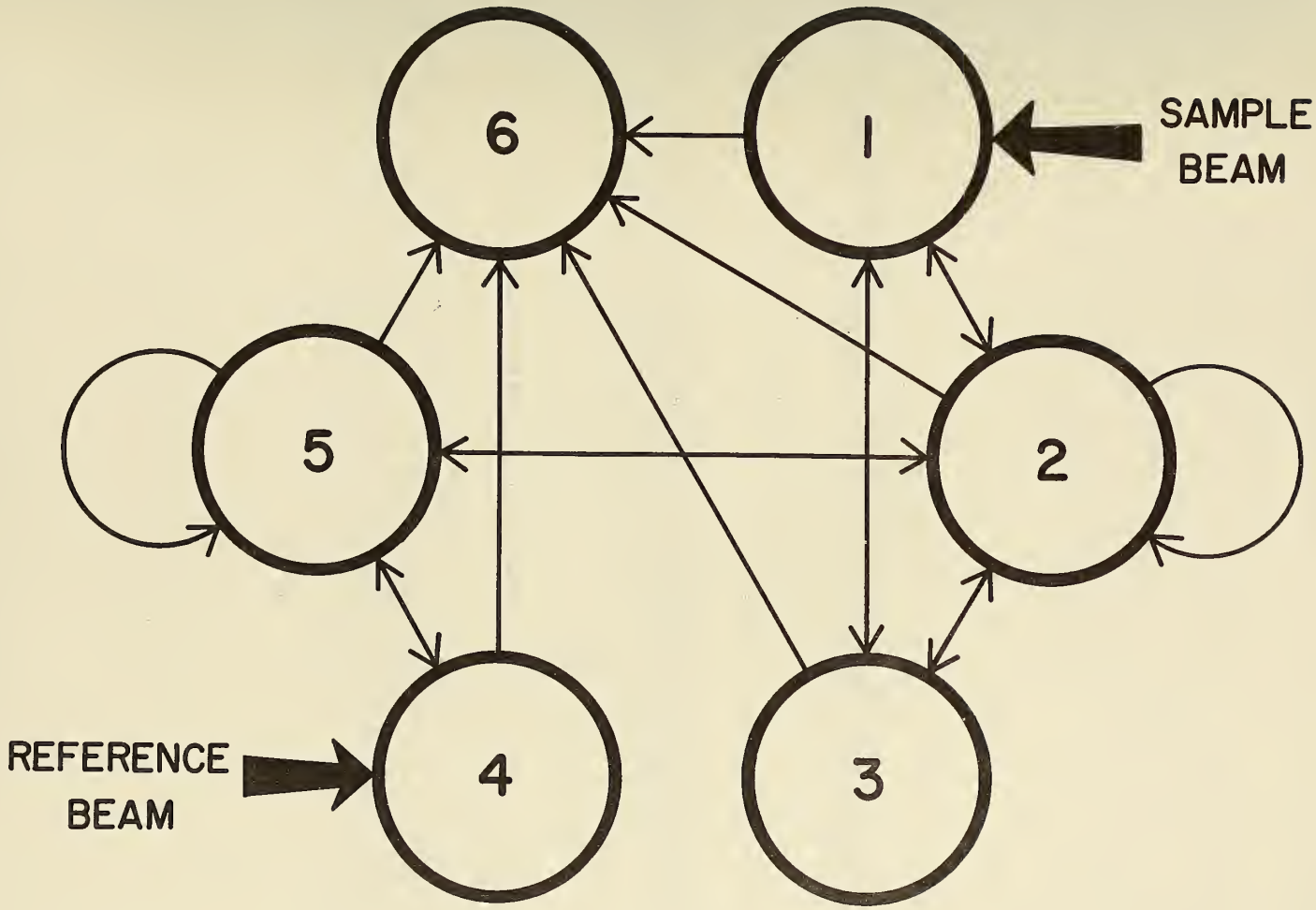

Figure 12. Schematic radiation transfer diagram for the sphere with baffle as shown in figure 11.

$$N_x = \eta_x \sum_{n=1}^{5} V_{n6} L_{xn} = \phi_1 \rho_x \eta_x (0.9989 + 0.0011\ \rho_x') \tag{E12}$$

where it has been assumed that $\rho_w = 1$. In a similar fashion the flux balance equations can be calculated for the case in which the incoming beam of radiation strikes region 4.

$$\pi A_1 L_{w1} = (V_{12} L_{w2} + V_{13} L_{w3})\ \rho_w' \tag{E13}$$

$$\pi A_2 L_{w2} = (V_{12} L_{w1} + V_{22} L_{w2} + V_{23} L_{w3} + V_{25} L_{w5})\ \rho_w \tag{E14}$$

$$\pi A_3 L_{w3} = (V_{13} L_{w1} + V_{23} L_{w2})\ \rho_w \tag{E15}$$

$$\pi A_4 L_{w4} = (\phi_2 + V_{45} L_{w5})\ \rho_w \tag{E16}$$

$$\pi A_5 L_{w5} = (V_{25} L_{w2} + V_{45} L_{w4} + V_{55} L_{w5})\ \rho_w \tag{E17}$$

From the L_{wn} determined by simultaneous solution of these equations, the signal N_w corresponding to the reference beam can be calculated as

$$N_w = \eta_x \sum_{n=1}^{5} V_{n6} L_{wn} = \phi_2 \rho_w \eta_x (0.99997 + 0.00003 \rho_x') \tag{E18}$$

where it has been assumed that after initial reflection $\rho_w = 1$. Comparing eqs. (E12) and (E18) with eqs. (A9) and (A10) respectively, it can be determined from eq. (A11) that

$$A_1 = .9989 \text{ and } G_1 = .0011 \tag{E19}$$

From the crudeness of the approximations used, this value for G_1 may be in error by as much as a factor of two.

APPENDIX F

Estimating Error Due to Angular Dependence of Response

The amount of error introduced by the entrance port and the painted ring around the sample port as discussed in section III.A.4.d depends upon the details of the specific scattering functions S_x and S_y of the samples x and y being compared. However, general cases can be treated in a way which will permit the magnitude of the errors introduced by the entrance port and the painted ring to be estimated. The scattering function S_x can be regarded as being the sum of two parts, S_{sx} which describes the Fresnel surface reflection and S_{bx} which describes the body reflection due to scattering which takes place beneath the surface. These two components are quite naturally distinguished in the case of polished surfaces, but the choice of the separate functions becomes more arbitrary in the case of samples with rough surfaces. However, even a rather arbitrary division can be useful, and no first order error will be introduced as long as

$$S_{bx} + S_{sx} = S_x \tag{F1}$$

1. Surface Reflection

The surface reflected component is not strongly chromatic but depends strongly on the texture of the surface. A function representative of the commonly occurring angular dependence of S_{sx} is:

$$S_{sx}(\vec{u}) = \rho_{sx} r(k) e^{-k\beta^2} \tag{F2}$$

where ρ_{sx} is the total surface reflectance at the given angle of incidence and β is the angle between the direction of emergence $\vec{u}$ and the direction of specular reflection which would occur if the sample were replaced by a plane mirror. The constant r(k) is a normalization constant which will be chosen so that

$$\int r(k) e^{-k\beta^2} \, d\omega = 1 \tag{F3}$$

when the integral is taken over the entire hemisphere. Since this is only a generalized model, since the angle of incidence is nearly normal, and since the response is polarization insensitive, it was felt to be unnecessary to include the details of polarization effects in the model for the purpose of estimating the measurement errors which are introduced by differences between S_{sx} for different samples. With this model for S_{sx}, the fraction of the total surface reflected radiation which is lost out the port can be calculated as

$$F_p(G_x) = \int_p S_{sx} \vec{u} \cdot a \, d\omega / \rho_{sx} \tag{F4}$$

where the integral is taken over the entrance port, and the fraction of the total surface reflected radiation which strikes the painted ring is

$$F_r(G_x) = \int_r S_{sx} \vec{u} \cdot a \, d\omega / \rho_{sx} \tag{F5}$$

where the integral is taken over the painted ring. The argument G is the percent of the total surface reflected flux which falls within a 11.7° by 4.4° rectangular solid angle centered on the specular direction. (The solid angle defining G is arbitrarily chosen the same as that in a glossmeter measuring ASTM 60° gloss [14]. Thus, for dark colored dielectric materials, G is approximately the ASTM 60° gloss [14].) $F_p(G)$ and $F_r(G)$ are

shown in figure 13. $F_r(G)$ is approximately the same for both of the spheres, but $F_p(G)$ differs markedly between the 0° and 6° incidence spheres. From the surface component of reflection, the contribution ε_{sp} to ε_p as defined in eq. (10) is

$$\varepsilon_{sp} = \frac{\rho_{sy}}{\rho_y} F_p(G_y) - \frac{\rho_{sx}}{\rho_x} F_p(G_x) \tag{F6}$$

From the surface component of reflection, the contribution ε_{sr} to ε_r as defined in eq. (11) is

$$\varepsilon_{sr} = 0.15 \left[\frac{\rho_{sy}}{\rho_y} F_r(G_y) - \frac{\rho_{sx}}{\rho_x} F_r(G_x) \right] \tag{F7}$$

To obtain an estimate of the magnitude of errors which can result, the case in which $\rho_y < \rho_x$ will be considered. With non-metallic materials for which $\rho_{sy} \simeq \rho_{sx} \simeq .05$, it follows that the maximum possible ε_{sr} is $1.3 \times 10^{-4}/\rho_y$, which would occur when y was perfectly diffuse ($G_y = 0.49$) and $G_x > 1$. For the 6° incidence sphere, the largest possible value of ε_{sp} is $2 \times 10^{-3}/\rho_y$ which would occur when a low gloss sample y for which $G_y \simeq 10$ is being compared to a higher gloss sample x($G_x > 60$). In either case, when ρ_y is reasonably large, a correction based on using measured gloss values for G_x and G_y would reduce the errors to insignificance. On the other hand, ε_{sp} can be as great as $5 \times 10^{-2}/\rho_y$ for the 0° incidence sphere, and the uncertainty in ε_{sp} per gloss unit is approximately $5 \times 10^{-4}/\rho_y$. For this reason the 0° incidence sphere will generally be restricted to use with samples with flat highly polished surfaces ($G > 95$). Since the F_p curves are almost the same for both the 0° and 6° incidence spheres only for $G < 2$, a very matte sample will be used to calibrate the 0° sphere measurements using a standard which has been evaluated on the 6° sphere, or a very high gloss standard ($G > 95$) for which the surface reflectance ρ_s is known will be used.

As a final observation on the effects of the distribution of the surface reflected flux upon measurements, a curve is shown in figure 13 giving the fractional error in measuring ρ_s using a 0°/45° bidirectional reflectometer. As long as $G > 5$, the fractional error in measuring ρ_s is -1, i.e. the surface component of reflection is effectively excluded from all measurements of samples having $G > 5$. Relative measurements of the reflectance of such samples can be made in this mode with negligible effects due to surface reflection. However, this mode of measurement will not be used with samples in the transition range $5 > G > 1$, and it should not be used for dark colored samples when $G < 5$.

2. Body Reflection

A second contribution to ε_p and ε_r is due to differences between the body component of the reflection of samples x and y. For normal incidence, the generalized scattering function S_{bx} can be described as:

$$S_{bx}(\gamma) = \sum_{i=0}^{\infty} a_{ix} Z_i(\gamma) \tag{F8}$$

where the $Z_i(\gamma)$ are a complete orthonormal set of functions such that

$$\int Z_j(\gamma) \, Z_i(\gamma) \cos\gamma \sin\gamma \, d\gamma = \begin{cases} 0; & i \neq j \\ 1; & i = j \end{cases} \tag{F9}$$

and γ is the angle of emergence measured from the normal to the sample surface. Such a set can be written in terms of functions resembling spherical harmonics in 2γ, and since most of the detailed structure of the total radiance distribution can be attributed to surface reflectance, the angular variation of the body reflection can be represented in most cases by the first three terms of eq. (F8) where

$$Z_0(\gamma) = \sqrt{1/\pi} \tag{F10}$$

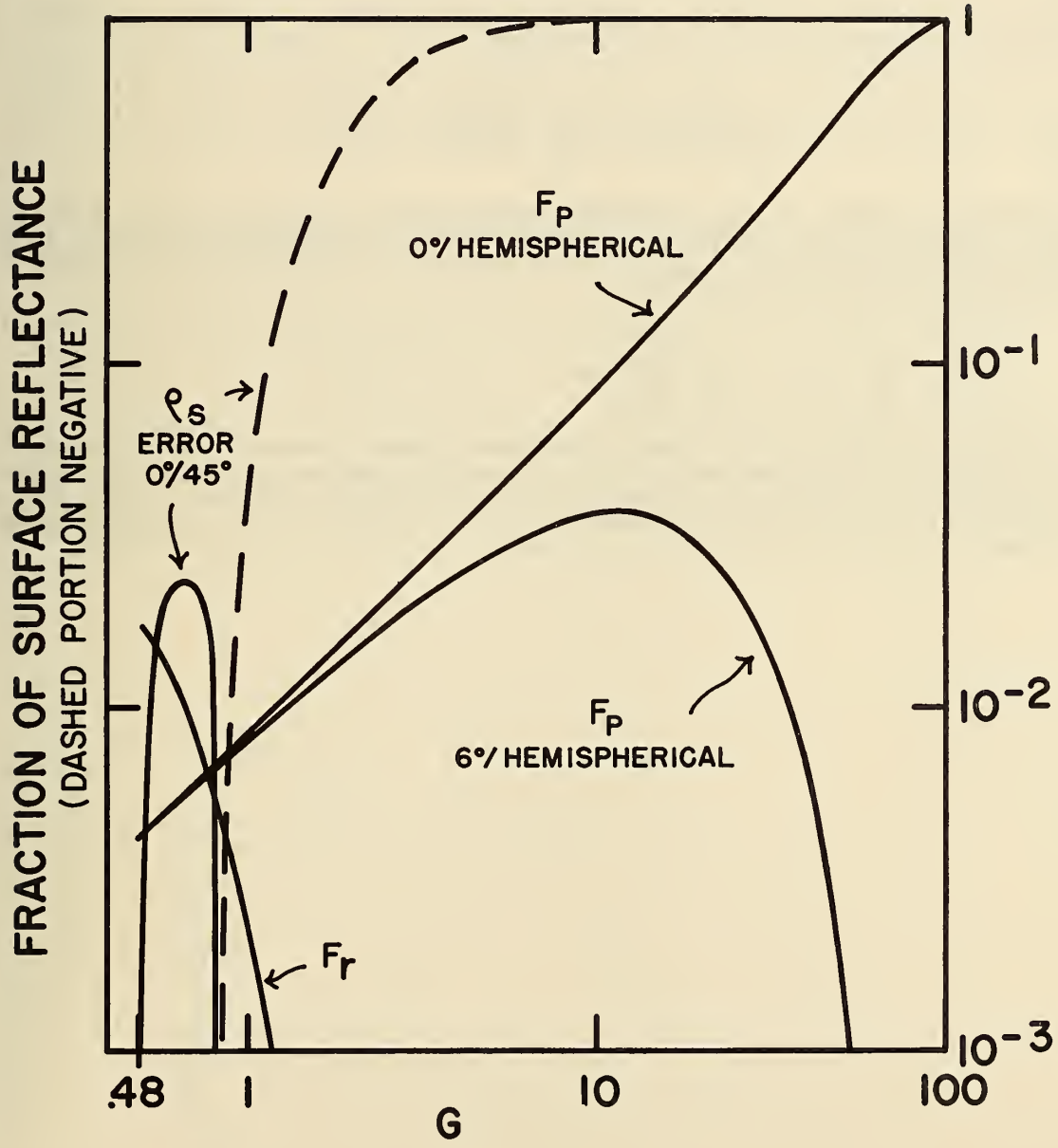

Figure 13. Data to be used in calculating errors due to differences in distributions of surface reflected radiation as described in appendix F.

$$Z_1(\gamma) = \sqrt{3/\pi}\cos 2\gamma \qquad \text{(F11)}$$

$$Z_2(\gamma) = \sqrt{5/4\pi}\,(3\cos^2(2\gamma) - 1) \qquad \text{(F12)}$$

With the entrance port subtending 0.013 sr at $\gamma \simeq 0$, one obtains ε_{bp}, the body reflection portion of ε_p, from eq. (10) as

$$\varepsilon_{bp} = 1.3 \times 10^{-2}\left[\sqrt{\frac{3}{\pi}}\left(\frac{a_{1y}}{\rho_y} - \frac{a_{1x}}{\rho_x}\right) + \sqrt{\frac{5}{\pi}}\left(\frac{a_{2y}}{\rho_y} - \frac{a_{2x}}{\rho_x}\right)\right]$$

with the painted ring of reflectance 0.85 subtending 0.055 sr at $\gamma \simeq \pi/2$, one obtains ε_{br}, the body reflection part of ε_r, from eq. (11) as

$$\varepsilon_{br} = -8.3 \times 10^{-3}\left[\sqrt{\frac{3}{\pi}}\left(\frac{a_{1y}}{\rho_y} - \frac{a_{1x}}{\rho_x}\right) - \sqrt{\frac{5}{\pi}}\left(\frac{a_{2y}}{\rho_y} - \frac{a_{2x}}{\rho_x}\right)\right]$$

The magnitude of these contributions depend upon a_{1x}, a_{2x}, a_{1y} and a_{2y}, which can be determined from bidirectional reflectance measurements made at the angles of viewing at which $Z_1(\gamma)$ and $Z_2(\gamma)$ go to zero. If reflecting surfaces x and y have the same goniometric distribution of reflected radiation,

$$\frac{a_{1x}}{\rho_x} = \frac{a_{1y}}{\rho_y} \quad \text{and} \quad \frac{a_{2x}}{\rho_x} = \frac{a_{2y}}{\rho_y}$$

and that both ε_{bp} and ε_{br} will be zero. One rather common occurrence in highly absorbing diffuse reflectors is for the body reflected radiation to be concentrated toward the surface normal, thereby resulting in a relatively large positive $Z_1(\gamma)$ component. Although ε_{bp} and ε_{br} tend to cancel under these circumstances, the cancellation is not complete and such measurements must be treated with special caution.

APPENDIX G

Focusing the Exit Slit Optics

Because the width (up to 3 mm) of the exit slit is significant compared to the focal length (178 mm) of the off-axis parabolic mirror in the exit slit optics, it is not practical to collimate the exit beam in the usual sense in which the exit slit is placed at the focus of the off-axis parabolic mirror. If this were done, the beam of radiation would diverge strongly, nearly doubling in its dimensions in going from the off-axis parabolic mirror to the experiment location. Instead, an image of the exit slit is formed at such a distance that the dimensions of the image and the dimensions of the illuminated area of the off-axis parabolic mirror are approximately the same. A simplified schematic optical diagram of this arrangement is shown in figure 14, where, for clarity the off-axis parabolic mirror is represented schematically as a lens and the beam-deflecting plane mirrors have been omitted. It can be seen from the figure that over the entire distance D, the radiation is confined to approximately a constant cross section, although the distribution of the radiation across the cross section differs at different locations along this path. With the instrument set for a 10 nm half-height bandpass (1.5 mm slit width) and adjusted for the conditions shown in figure 14, the distance D is approximately 1.4 meters and the distance d is approximately .4 meters.

The plane P in which the image of the monochromator exit mirror lies is of particular interest. At this location, the beam cross section is sharply defined and, in the ideal case of perfect optics, the spectral irradiance is independent of location within the cross section. At the location of the image of the exit slit, the spectral irradiance distribution is shifted by one half-height bandwidth from one side of the exit slit image to the other. For most of the experiments which are conducted with this instrument, it would be ideal if the sample could be located in plane P. However, because of the size of the accessory apparatus, in most of the measurements the sample is located at or just a little beyond the image of the exit slit. For this reason, when a sample is measured for which the uniformity of the spectral reflectance across the surface is suspect, the sample will be measured, rotated 180°, and remeasured in order to ascertain the effect of the coupling between the shift in spectral irradiance distribution across the beam and the non-uniformity in sample reflectance across the beam.

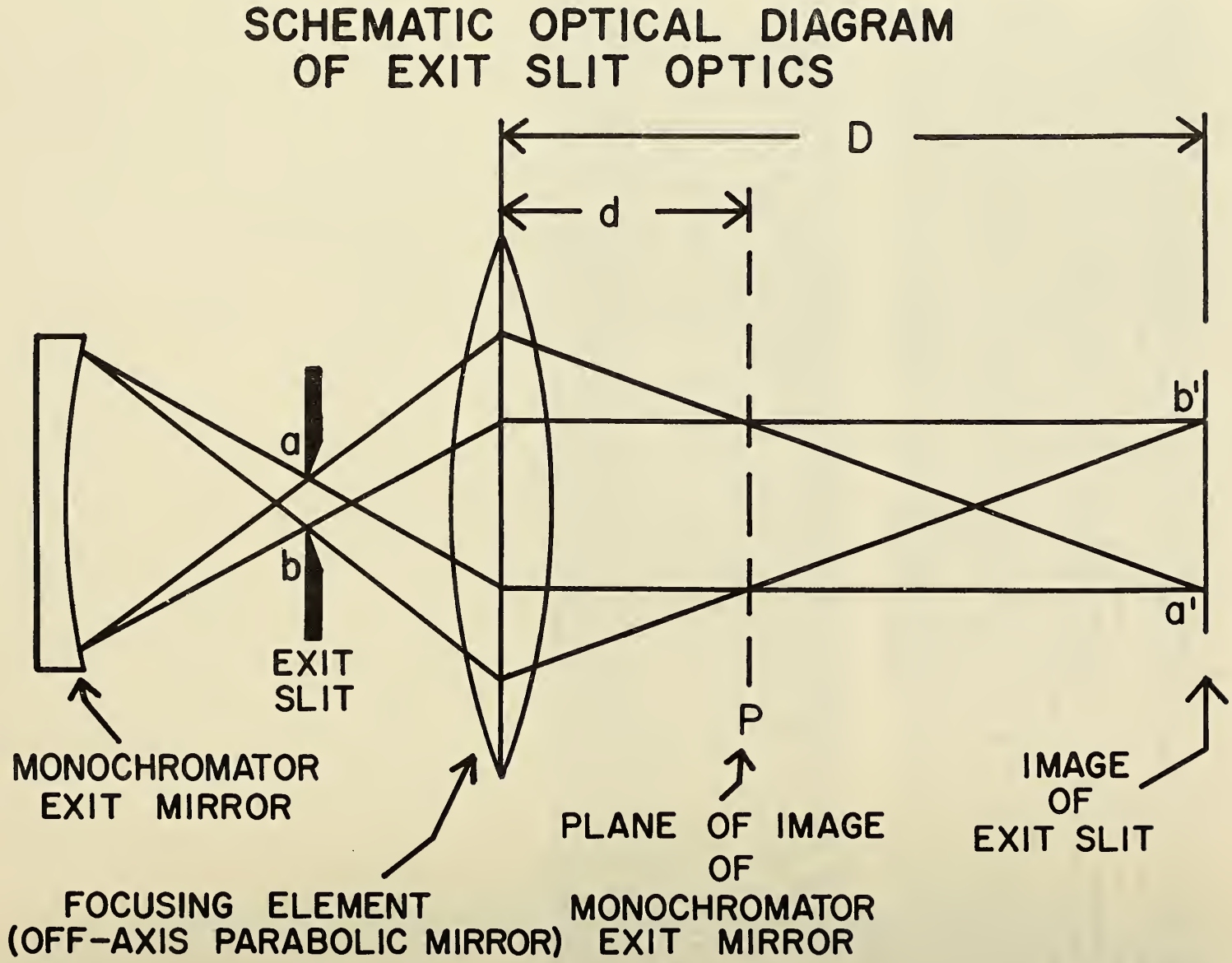

Figure 14. Schematic optical diagram of exit slit optics.

V. REFERENCES

1. Certain commercial materials are identified in this Technical Note in order to specify adequately the procedure. In no case does such identification imply endorsement or evaluation by the National Bureau of Standards.

2. Popenoe, C.H. and Campbell, M.C., "MIDAS Modular Interactive Data Acquisition System — Description and Specification", NBS Tech. Note No. 790 (August 1973).

3. Tests performed by Dr. John M. Jerke, Optics and Micrometrology Section, Optical Physics Division, National Bureau of Standards.

4. Mielenz, K.D. and Eckerle, K.L., "Design, Construction, and Testing of a New High Accuracy Spectrophotometer", NBS Tech. Note No. 729 (June 1972).

5. Keegan, H.J. and Gibson, K.S., "On the Use of Working Standards of Didymium and Vitrolite Glasses for Spectrophotometric Measurements", J. Opt. Soc. Am. 34 (12), 770 (1944).

6. Keegan, H.J., Schleter, J.C., and Judd, D.B., "Glass Filters for Checking Performance of Spectrophotometer — Integrator System of Color Measurement", J. Res. NBS. 66A (3), 203 (June 1962).

7. Eckerle, K.L., Venable, W.H., Jr., and Weidner, V.R., "Averaging Sphere for Ultraviolet, Visible, and Near Infrared Wavelengths: A Highly Effective Design:, Appl. Opt. 15 (3), 703 (March 1976).

8. Grum, F. and Saltzman, M., "New White Standard of Reflectance", presented at the 18th session of CIE, London, England in September 1975.

9. Venable, William H., Jr., and Hsia, Jack J., "Optical Radiation Measurements: Describing Spectrophotometric Measurements", NBS Tech. Note No. 594-9 (November 1974).

10. Mielenz, K.D. and Eckerle, K.L., "Spectrophotometer Linearity Testing Using the Double-Aperture Method", Appl. Opt. 11 (10), 2294 (1972).

11. Goebel, D.G., Caldwell, B.P., Hammond, H.K. III, "Use of an Auxiliary Sphere with a Spectroreflectometer to Obtain Absolute Reflectance", J. Opt. Soc. Am. 56 (6), 783 (June 1966).

12. Van den Akker, J.A., Dearth, L.R., and Shillcox, W.M., "Evaluation of Absolute Reflectance for Standardization Purposes", J. Opt. Soc. Am. 56 (2), 250 (February 1966).

13. Jacquez, J.A. and Kuppenheim, H.F., "Theory of the Integrating Sphere", J. Opt. Soc. Am. 45 (6), 460 (1955).

14. ASTM Designation: D523-67(1972), Standard Method of Test for Specular Gloss, Annual Book of ASTM Standards Part 27 (1974).

NBS-114A (REV. 7-73)

U.S. DEPT. OF COMM. BIBLIOGRAPHIC DATA SHEET	1. PUBLICATION OR REPORT NO. NBS TN 594-11	2. Gov't Accession No.	3. Recipient's Accession No.

4. TITLE AND SUBTITLE

OPTICAL RADIATION MEASUREMENTS:
Development of an NBS Reference Spectrophotometer for Diffuse Transmittance and Reflectance

5. Publication Date October 1976

6. Performing Organization Code

7. AUTHOR(S)
William H. Venable, Jr., Jack J. Hsia, and Victor R. Weidner

8. Performing Organ. Report No.

9. PERFORMING ORGANIZATION NAME AND ADDRESS

NATIONAL BUREAU OF STANDARDS
DEPARTMENT OF COMMERCE
WASHINGTON, D.C. 20234

10. Project/Task/Work Unit No.

11. Contract/Grant No.

12. Sponsoring Organization Name and Complete Address *(Street, City, State, ZIP)*

Same

13. Type of Report & Period Covered Final

14. Sponsoring Agency Code

15. SUPPLEMENTARY NOTES

16. ABSTRACT *(A 200-word or less factual summary of most significant information. If document includes a significant bibliography or literature survey, mention it here.)*

A new reference spectrophotometer, designed primarly for the analysis of diffuse transmittance and reflectance, has been developed in the Institute for Basic Standards at NBS. The spectrophotometer consists of a broad band monochromator with optional bandpasses of 2, 5, 10, and 20 nanometers. The exit aperture of the monochromator is provided with special mirror optics to collimate and switch the beam for optional use as a reference or sample beam. These collimated beams are directed into a dark room where a variety of sample mounts, light gathering devices, and detectors can be installed. Measurements for which provisions have been made or are planned include directional-hemispherical reflectance of solids, liquids, and powders, directional-hemispherical reflectance as a function of angle of incidence, diffuse transmittance, haze, and bidirectional reflectance factor. This technical note describes the design of the instrument in detail, and gives the results of the performance tests and detailed error analyses which have been carried out to date.

17. KEY WORDS *(six to twelve entries; alphabetical order; capitalize only the first letter of the first key word unless a proper name; separated by semicolons)*

Bidirectional reflectance factor; diffuse reflectance; diffuse transmittance; reflectance; spectrophotometry.

18. AVAILABILITY [XXX] Unlimited

[ ] For Official Distribution. Do Not Release to NTIS

[x] Order From Sup. of Doc., U.S. Government Printing Office Washington, D.C. 20402, SD Cat. No. C13.46:594-11

[ ] Order From National Technical Information Service (NTIS) Springfield, Virginia 22151

19. SECURITY CLASS (THIS REPORT) UNCLASSIFIED

21. NO. OF PAGES 47

20. SECURITY CLASS (THIS PAGE) UNCLASSIFIED

22. Price $1.15

USCOMM-DC 29042-P74

NBS TECHNICAL PUBLICATIONS

PERIODICALS

JOURNAL OF RESEARCH reports National Bureau of Standards research and development in physics, mathematics, and chemistry. It is published in two sections, available separately:

• Physics and Chemistry (Section A)
Papers of interest primarily to scientists working in these fields. This section covers a broad range of physical and chemical research, with major emphasis on standards of physical measurement, fundamental constants, and properties of matter. Issued six times a year. Annual subscription: Domestic, $17.00; Foreign, $21.25.

• Mathematical Sciences (Section B)
Studies and compilations designed mainly for the mathematician and theoretical physicist. Topics in mathematical statistics, theory of experiment design, numerical analysis, theoretical physics and chemistry, logical design and programming of computers and computer systems. Short numerical tables. Issued quarterly. Annual subscription: Domestic, $9.00; Foreign, $11.25.

DIMENSIONS/NBS (formerly Technical News Bulletin)—This monthly magazine is published to inform scientists, engineers, businessmen, industry, teachers, students, and consumers of the latest advances in science and technology, with primary emphasis on the work at NBS. The magazine highlights and reviews such issues as energy research, fire protection, building technology, metric conversion, pollution abatement, health and safety, and consumer product performance. In addition, it reports the results of Bureau programs in measurement standards and techniques, properties of matter and materials, engineering standards and services, instrumentation, and automatic data processing.

Annual subscription: Domestic, $9.45; Foreign, $11.85.

NONPERIODICALS

Monographs—Major contributions to the technical literature on various subjects related to the Bureau's scientific and technical activities.

Handbooks—Recommended codes of engineering and industrial practice (including safety codes) developed in cooperation with interested industries, professional organizations, and regulatory bodies.

Special Publications—Include proceedings of conferences sponsored by NBS, NBS annual reports, and other special publications appropriate to this grouping such as wall charts, pocket cards, and bibliographies.

Applied Mathematics Series—Mathematical tables, manuals, and studies of special interest to physicists, engineers, chemists, biologists, mathematicians, computer programmers, and others engaged in scientific and technical work.

National Standard Reference Data Series—Provides quantitative data on the physical and chemical properties of materials, compiled from the world's literature and critically evaluated. Developed under a world-wide program coordinated by NBS. Program under authority of National Standard Data Act (Public Law 90-396).

NOTE: At present the principal publication outlet for these data is the Journal of Physical and Chemical Reference Data (JPCRD) published quarterly for NBS by the American Chemical Society (ACS) and the American Institute of Physics (AIP). Subscriptions, reprints, and supplements available from ACS, 1155 Sixteenth St. N.W., Wash. D. C. 20056.

Building Science Series—Disseminates technical information developed at the Bureau on building materials, components, systems, and whole structures. The series presents research results, test methods, and performance criteria related to the structural and environmental functions and the durability and safety characteristics of building elements and systems.

Technical Notes—Studies or reports which are complete in themselves but restrictive in their treatment of a subject. Analogous to monographs but not so comprehensive in scope or definitive in treatment of the subject area. Often serve as a vehicle for final reports of work performed at NBS under the sponsorship of other government agencies.

Voluntary Product Standards—Developed under procedures published by the Department of Commerce in Part 10, Title 15, of the Code of Federal Regulations. The purpose of the standards is to establish nationally recognized requirements for products, and to provide all concerned interests with a basis for common understanding of the characteristics of the products. NBS administers this program as a supplement to the activities of the private sector standardizing organizations.

Consumer Information Series—Practical information, based on NBS research and experience, covering areas of interest to the consumer. Easily understandable language and illustrations provide useful background knowledge for shopping in today's technological marketplace.

Order **above** *NBS publications from: Superintendent of Documents, Government Printing Office, Washington, D.C. 20402.*

Order **following** *NBS publications—NBSIR's and FIPS from the National Technical Information Services, Springfield, Va. 22161.*

Federal Information Processing Standards Publications (FIPS PUBS)—Publications in this series collectively constitute the Federal Information Processing Standards Register. Register serves as the official source of information in the Federal Government regarding standards issued by NBS pursuant to the Federal Property and Administrative Services Act of 1949 as amended, Public Law 89-306 (79 Stat. 1127), and as implemented by Executive Order 11717 (38 FR 12315, dated May 11, 1973) and Part 6 of Title 15 CFR (Code of Federal Regulations).

NBS Interagency Reports (NBSIR)—A special series of interim or final reports on work performed by NBS for outside sponsors (both government and non-government). In general, initial distribution is handled by the sponsor; public distribution is by the National Technical Information Services (Springfield, Va. 22161) in paper copy or microfiche form.

BIBLIOGRAPHIC SUBSCRIPTION SERVICES

The following current-awareness and literature-survey bibliographies are issued periodically by the Bureau:

Cryogenic Data Center Current Awareness Service. A literature survey issued biweekly. Annual subscription: Domestic, $20.00; Foreign, $25.00.

Liquified Natural Gas. A literature survey issued quarterly. Annual subscription: $20.00.

Superconducting Devices and Materials. A literature survey issued quarterly. Annual subscription: $20.00. Send subscription orders and remittances for the preceding bibliographic services to National Bureau of Standards, Cryogenic Data Center (275.02) Boulder, Colorado 80302.

U.S. DEPARTMENT OF COMMERCE
National Bureau of Standards
Washington, D.C. 20234

OFFICIAL BUSINESS

Penalty for Private Use, $300

POSTAGE AND FEES PAID
U.S. DEPARTMENT OF COMMERCE
COM-215

SPECIAL FOURTH-CLASS RATE
BOOK